

BEAM DYNAMICS IN PROTON AND HEAVY-ION LINACS BASED ON SUPERCONDUCTING TECHNOLOGY

Petr Ostroumov
FNAL, January 29 2004

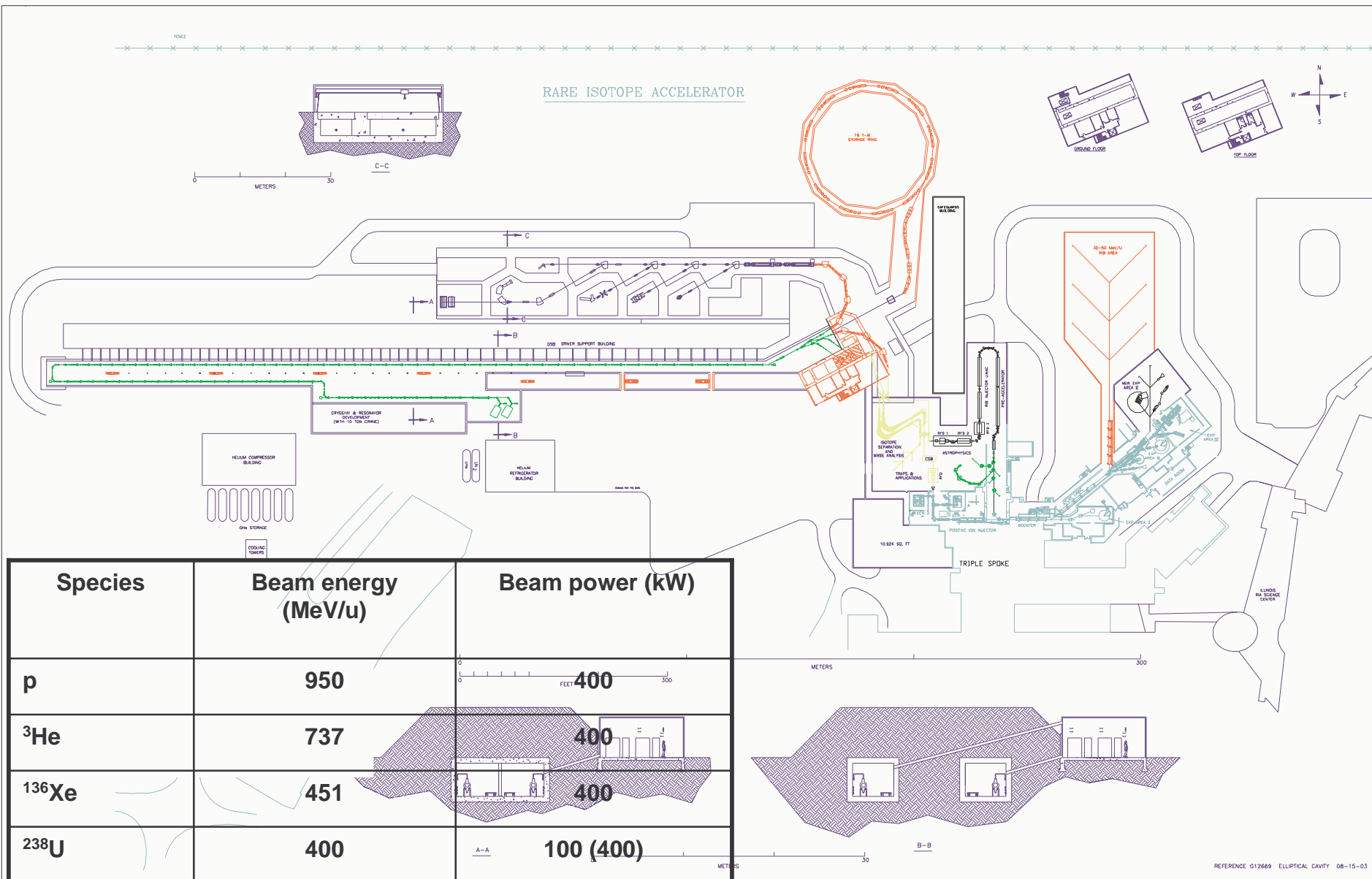
Argonne National Laboratory
Operated by The University of Chicago
for the U.S. Department of Energy



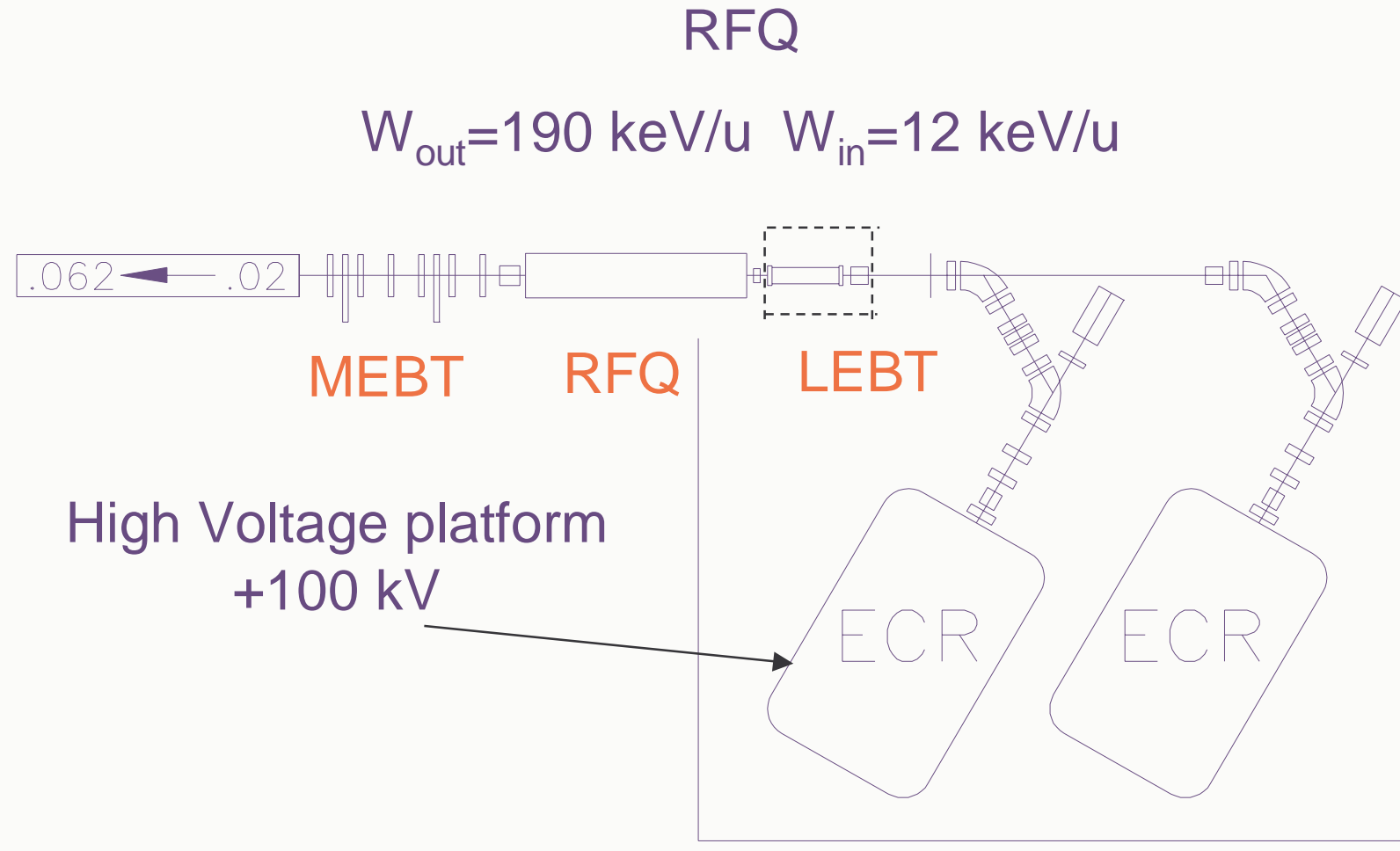
Outline

- Rare Isotope Accelerator: short introduction;
- 1.4 GV superconducting driver linac;
- Triple-spoke cavities vs elliptical one;
- Beam loss simulations;
- Spoke-loaded SC resonators in high-intensity proton/H-minus linacs;
- Two-frequency option of the 8 GeV H-minus linac.

What is the RIA?



Front End



RFQ resonant structure

$f=57.5$ MHz

$P=48$ kW

CW operation

q/A from 1/8 to 1.0

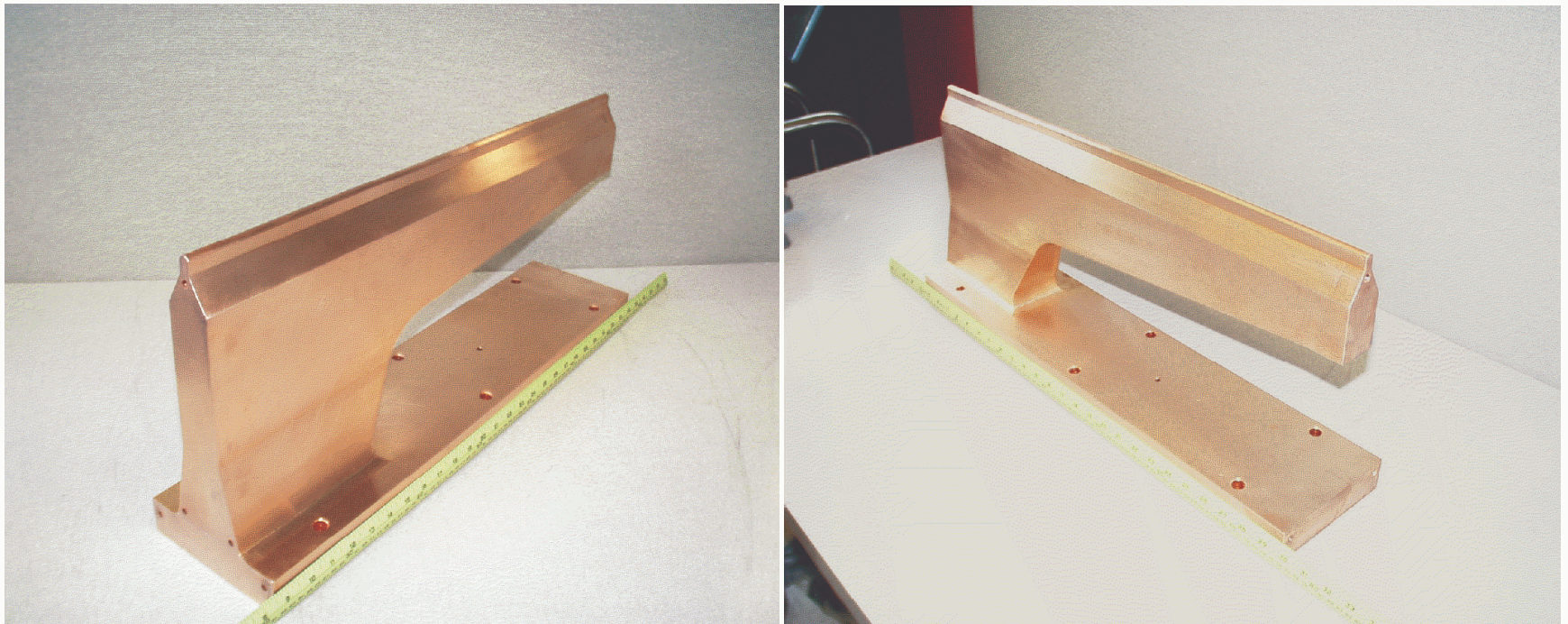
ϕ 49.5 cm

~ 4 m

Layer type = PEC



OFE copper vane brazed at ANL CMS

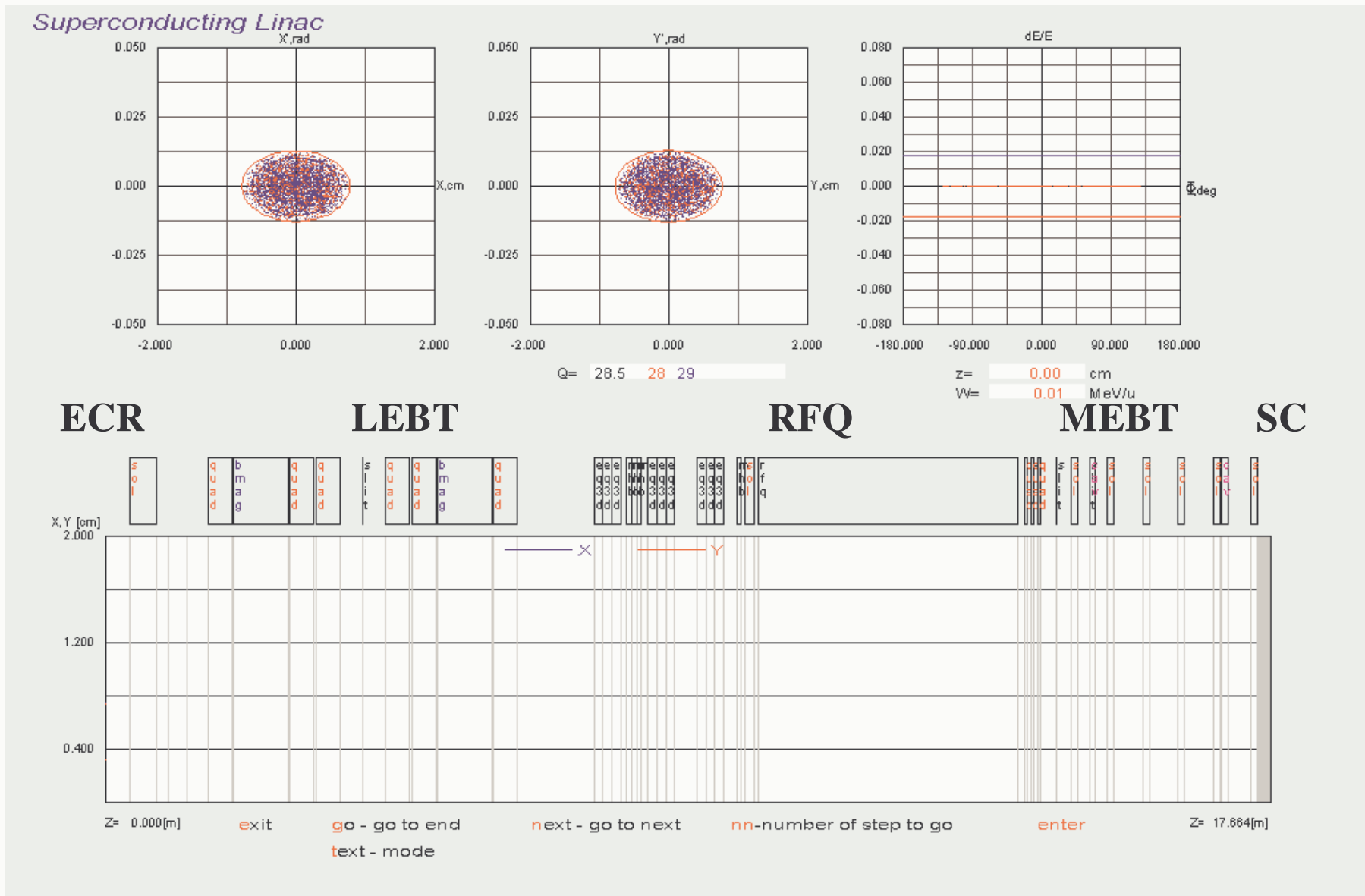


57.5 MHz, AI model, one segment

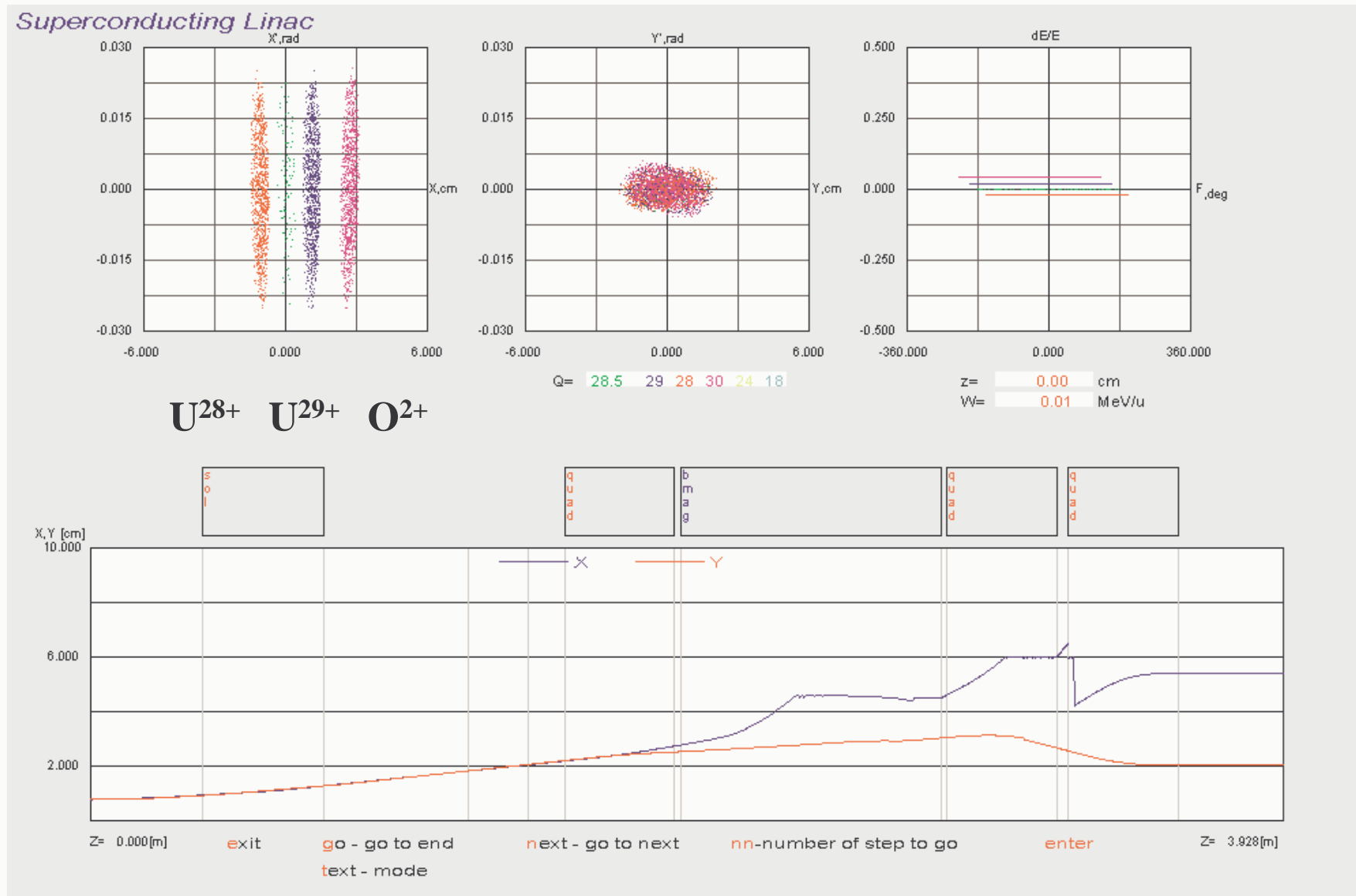
$Q_{\text{exp}} = 0.85 Q_{\text{sim}}$



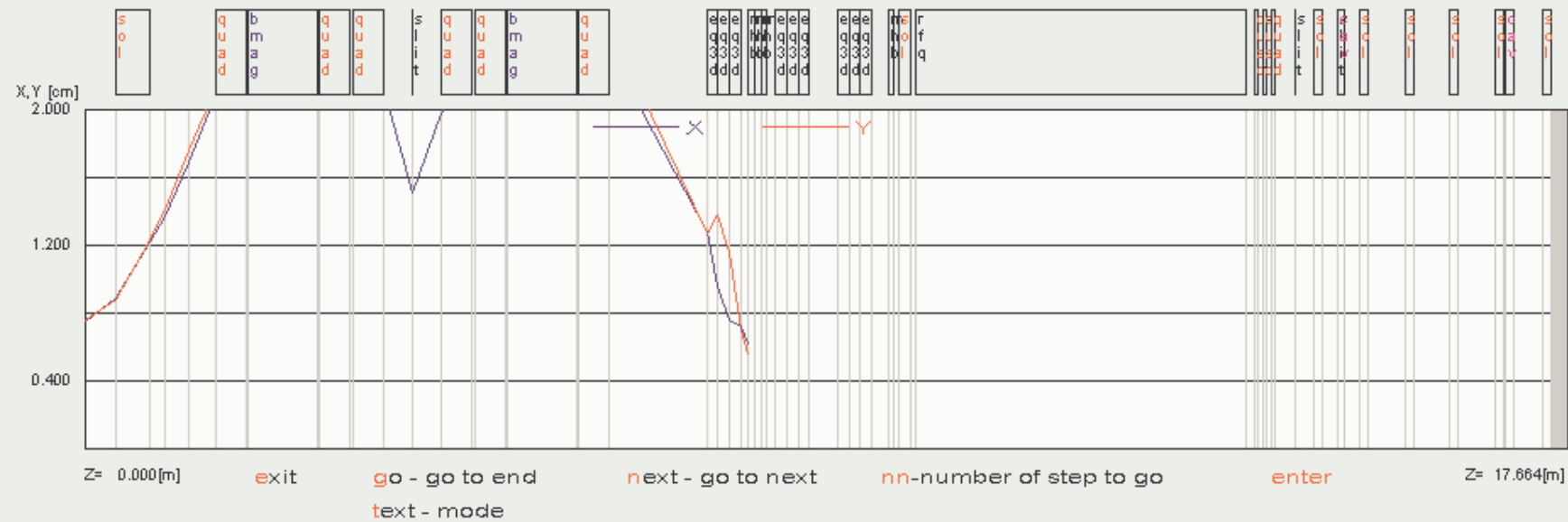
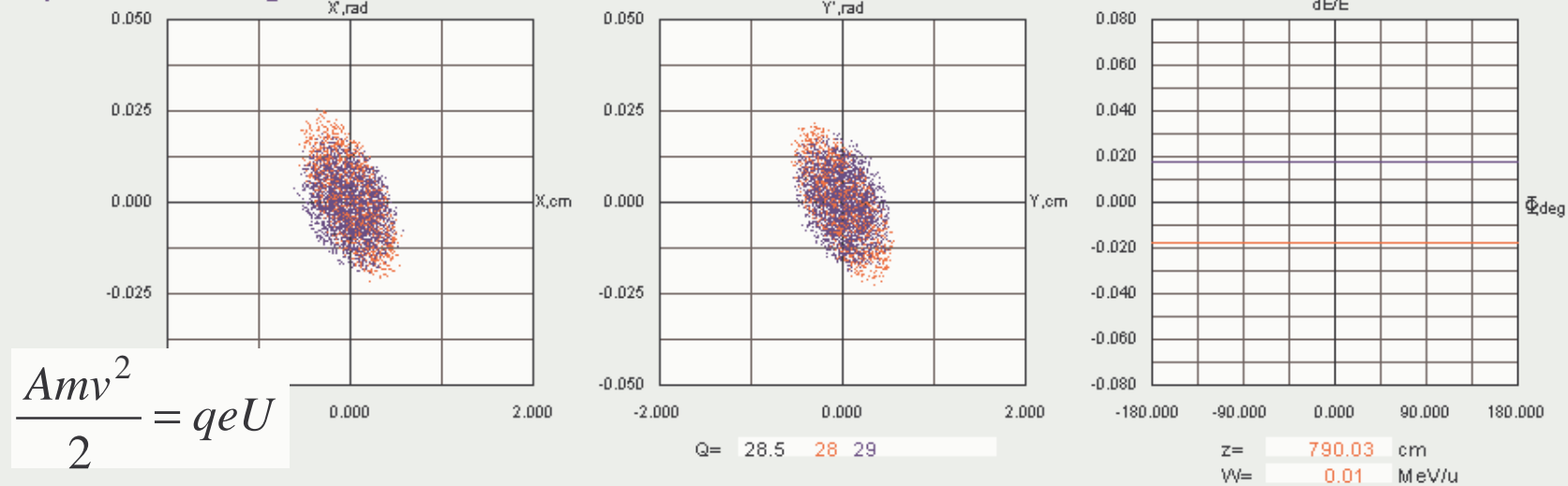
LEBT-RFQ-MEBT



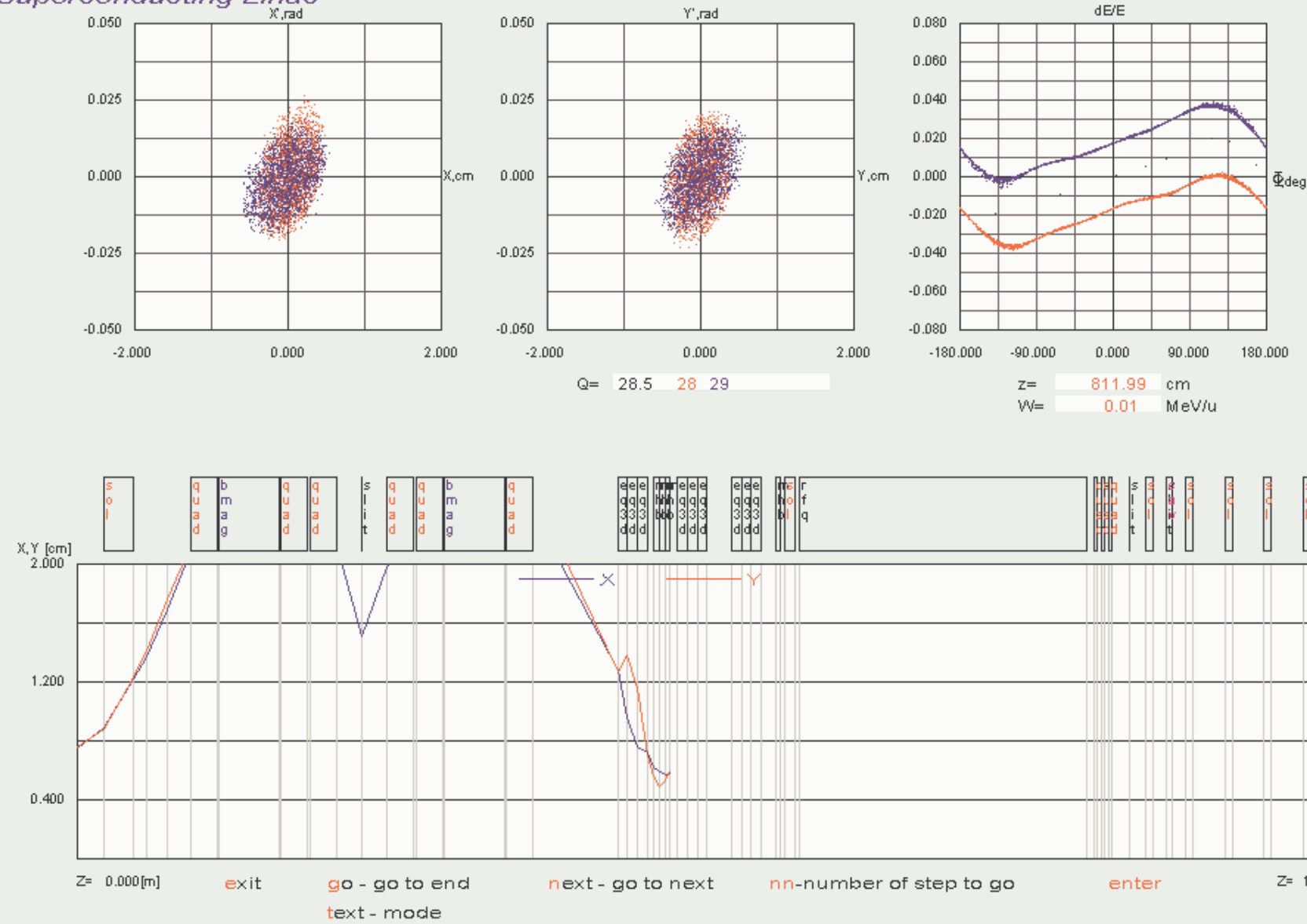
Charge selection



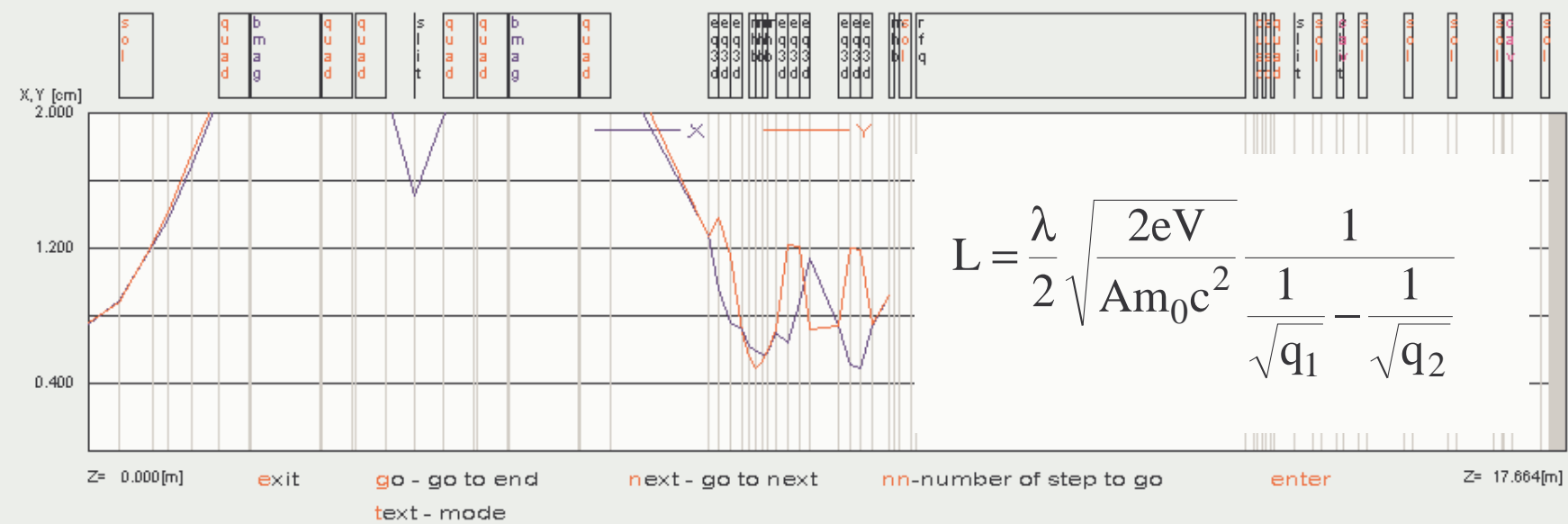
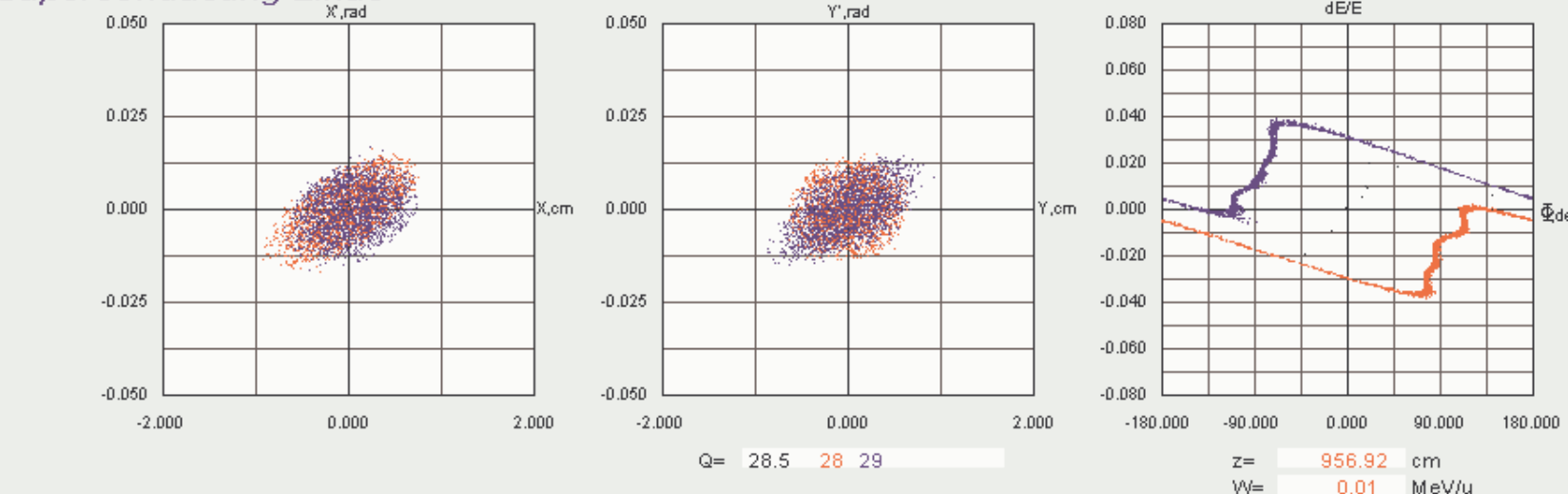
Superconducting Linac



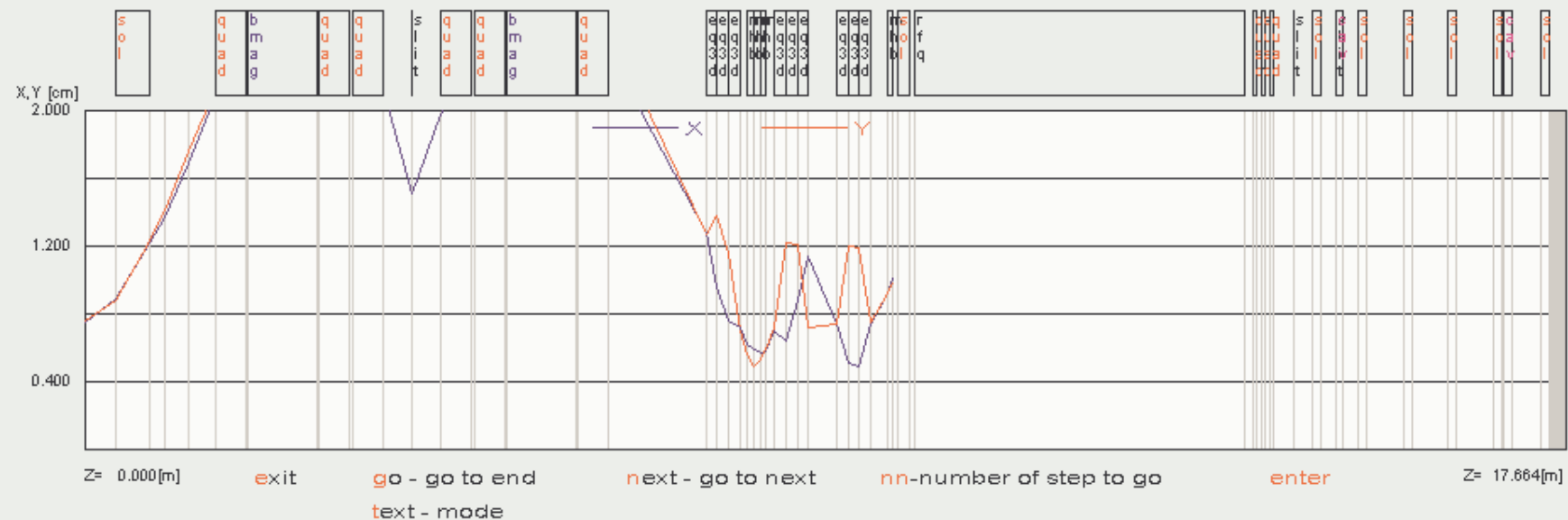
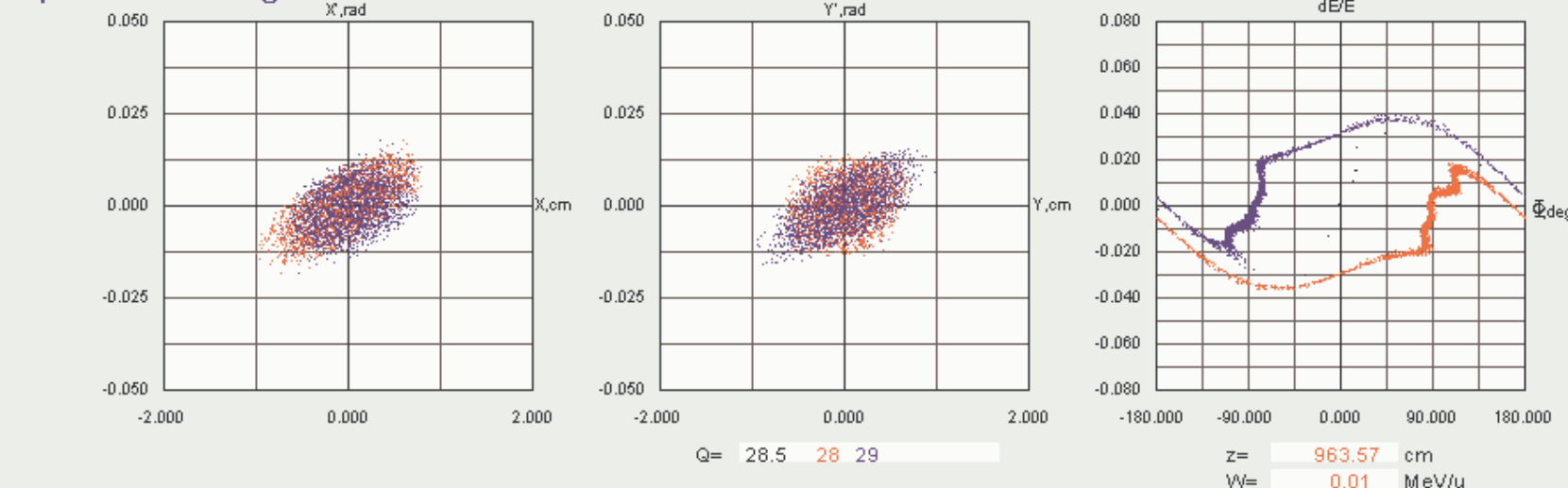
Superconducting Linac



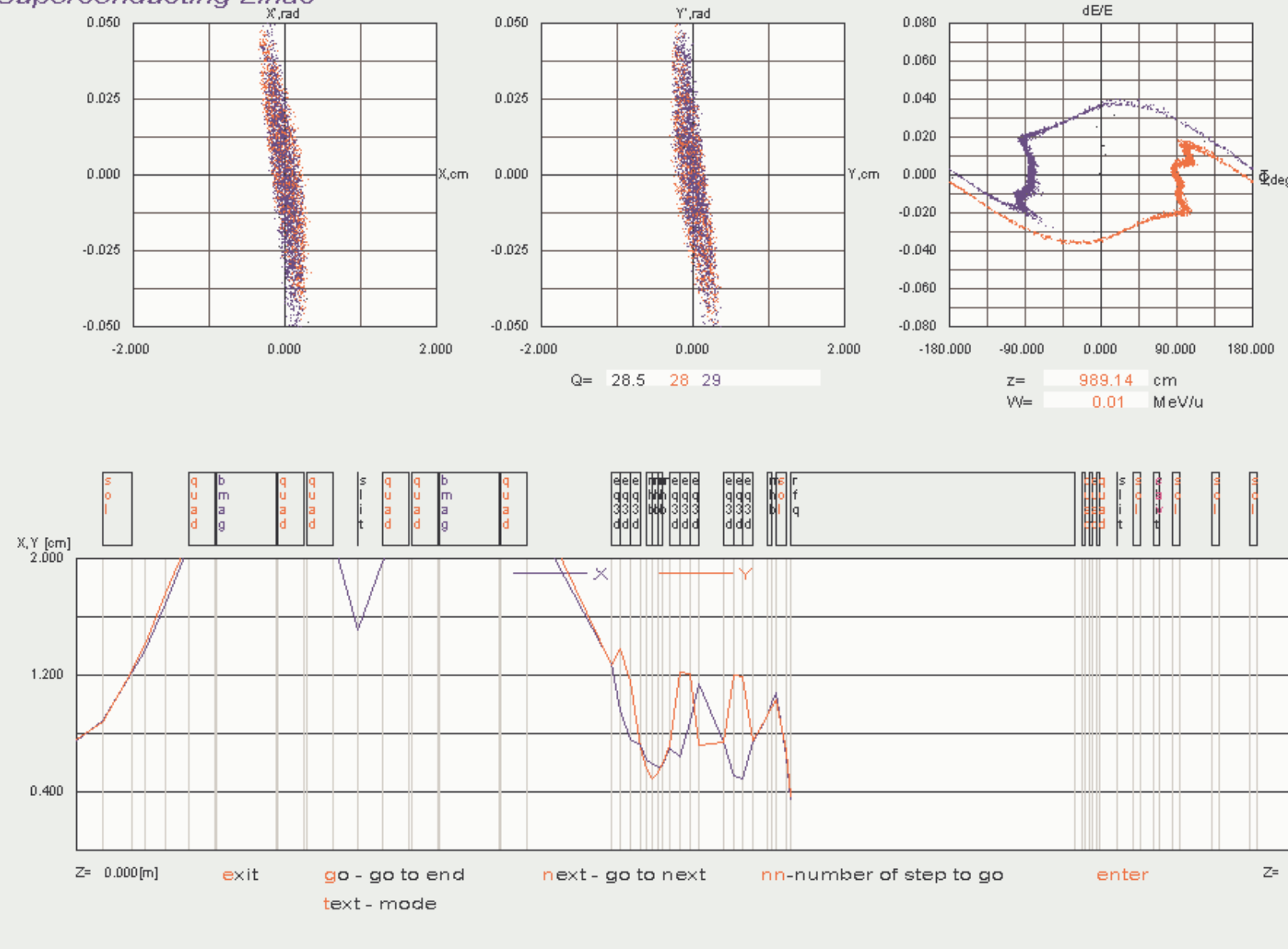
Superconducting Linac

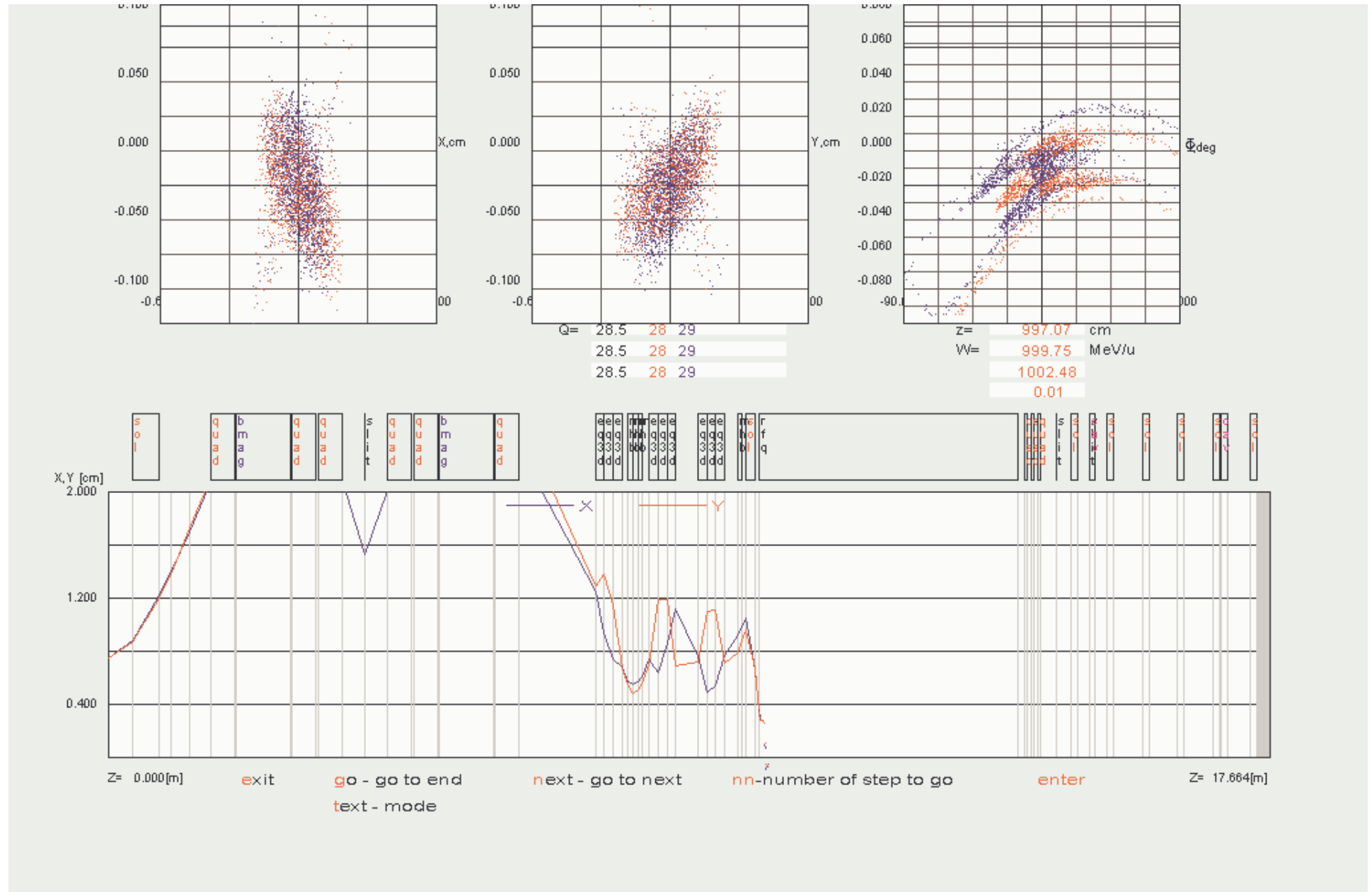


Superconducting Linac

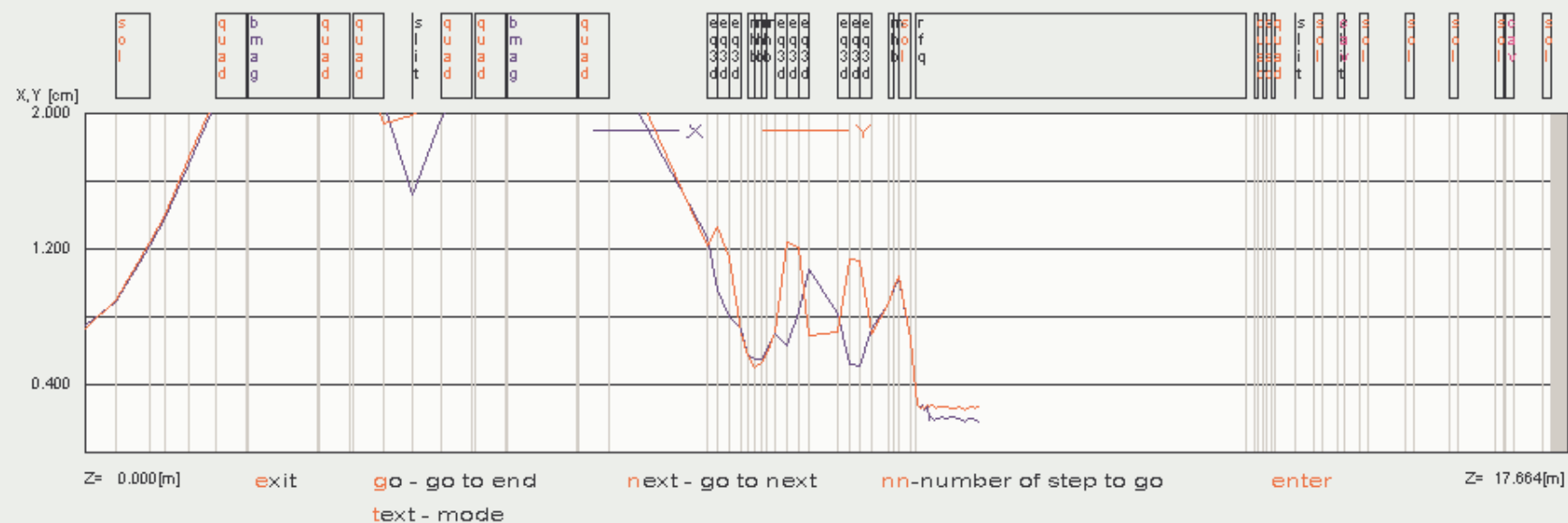
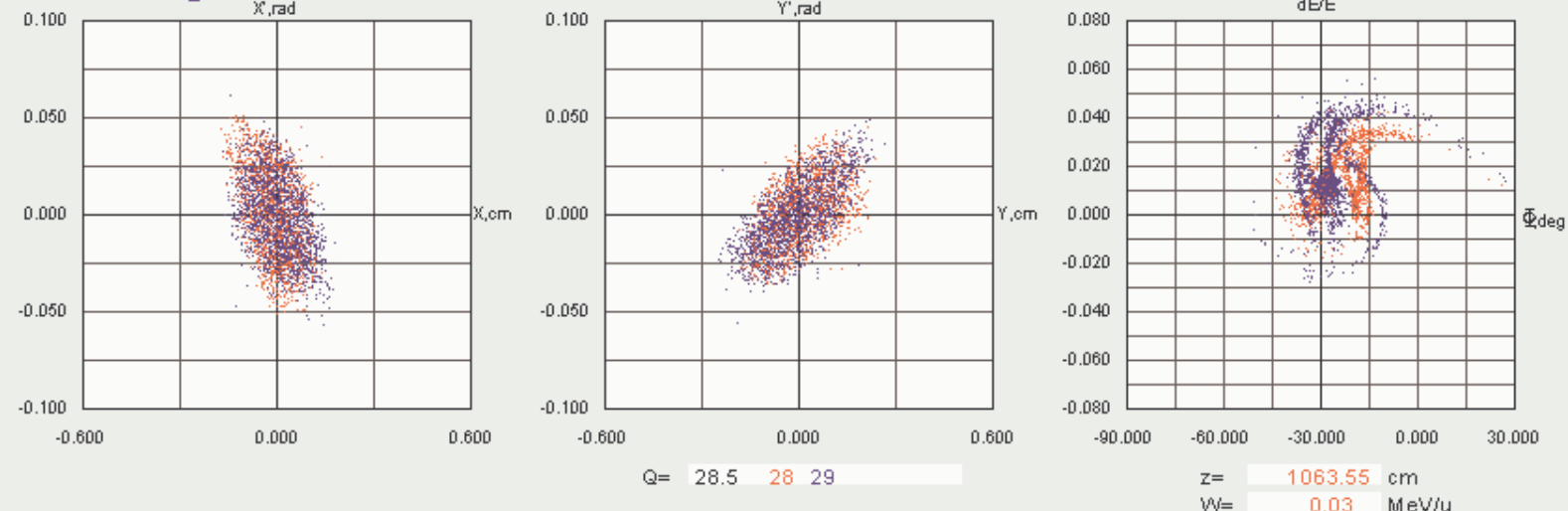


Superconducting Linac

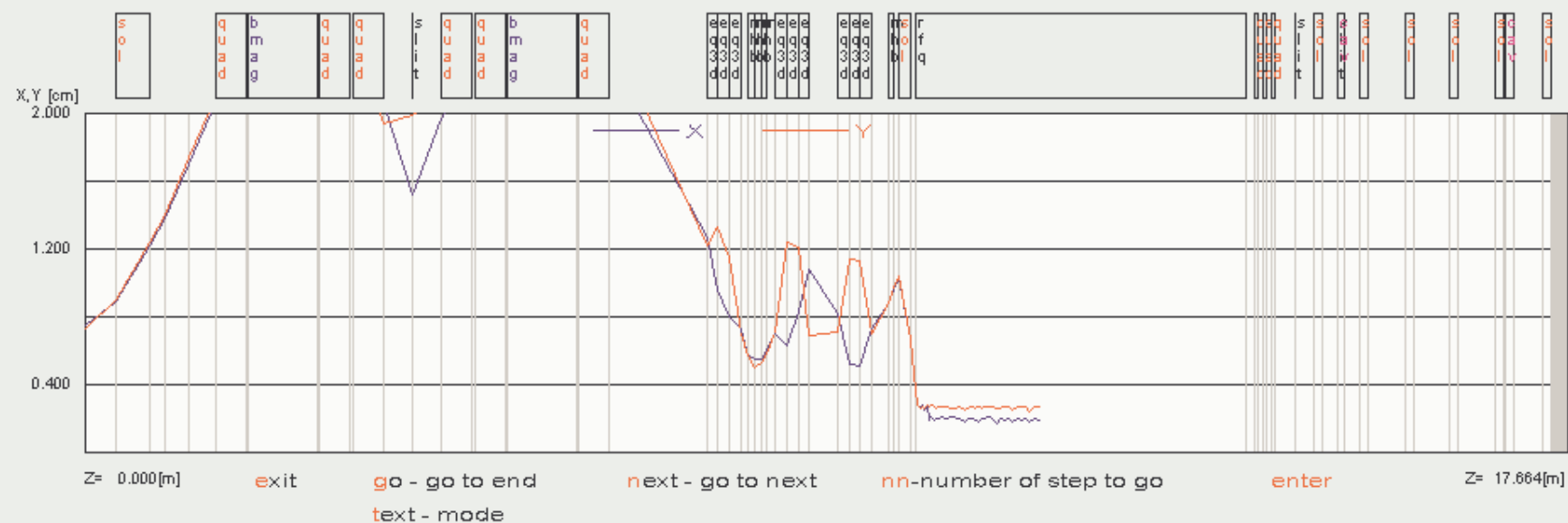
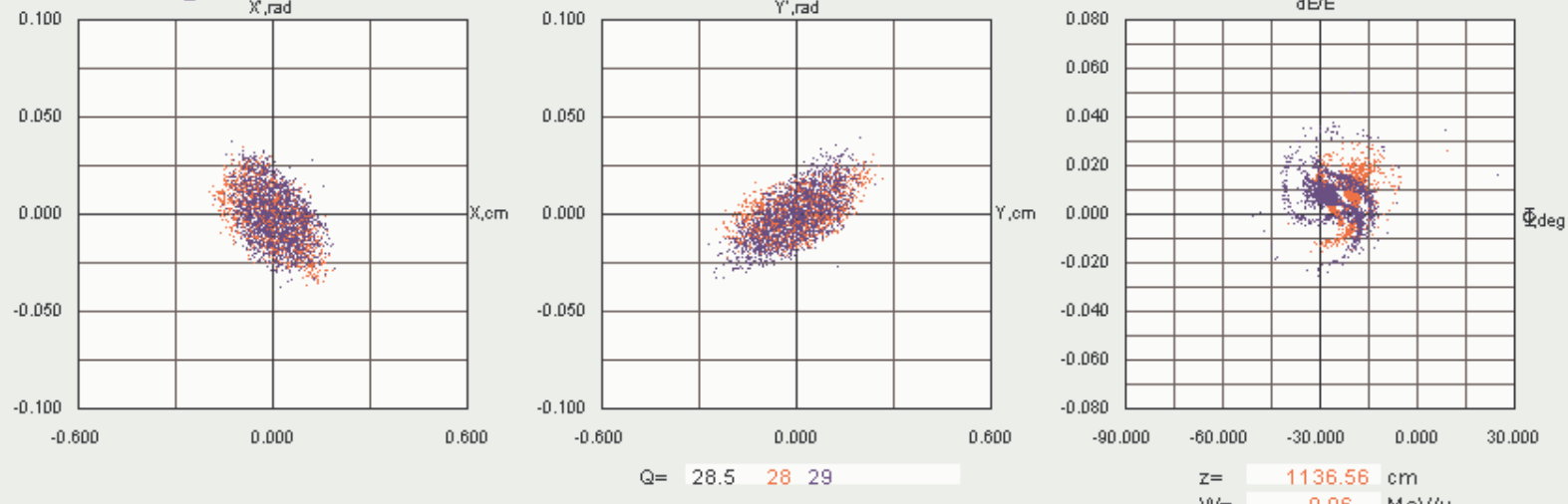




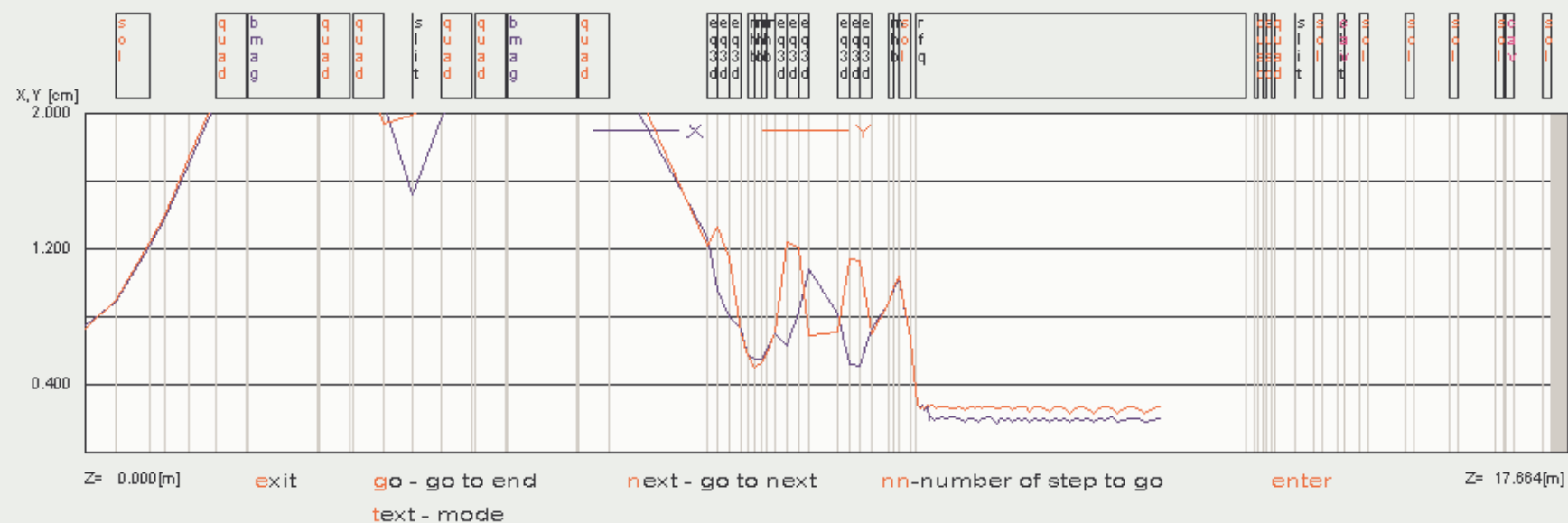
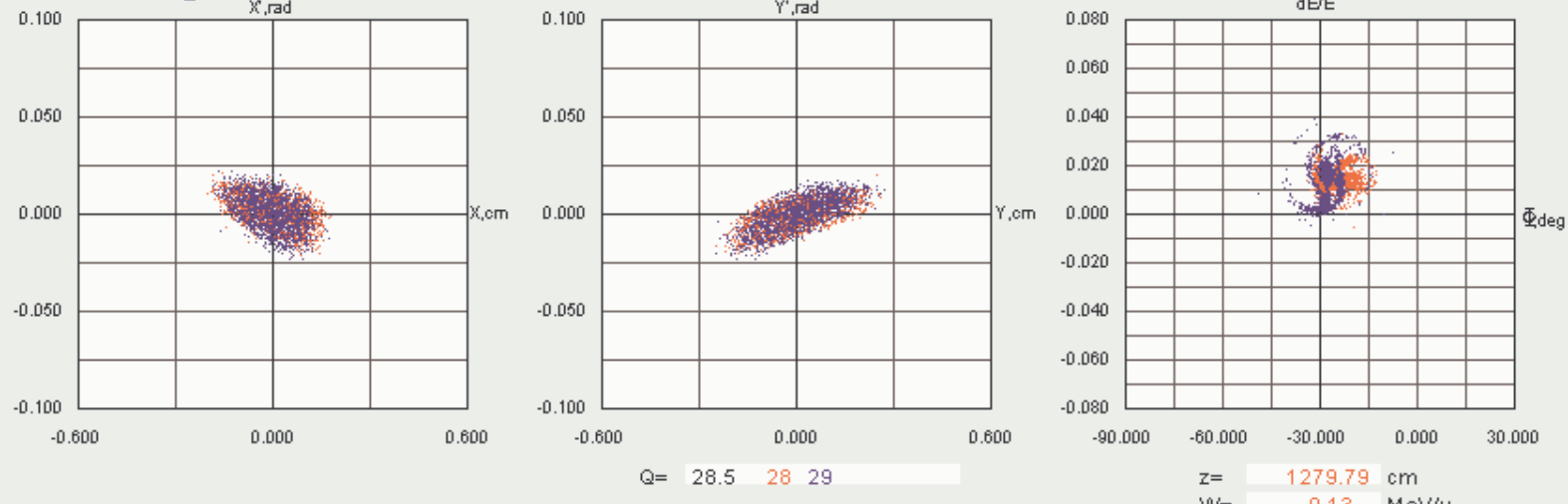
Superconducting Linac



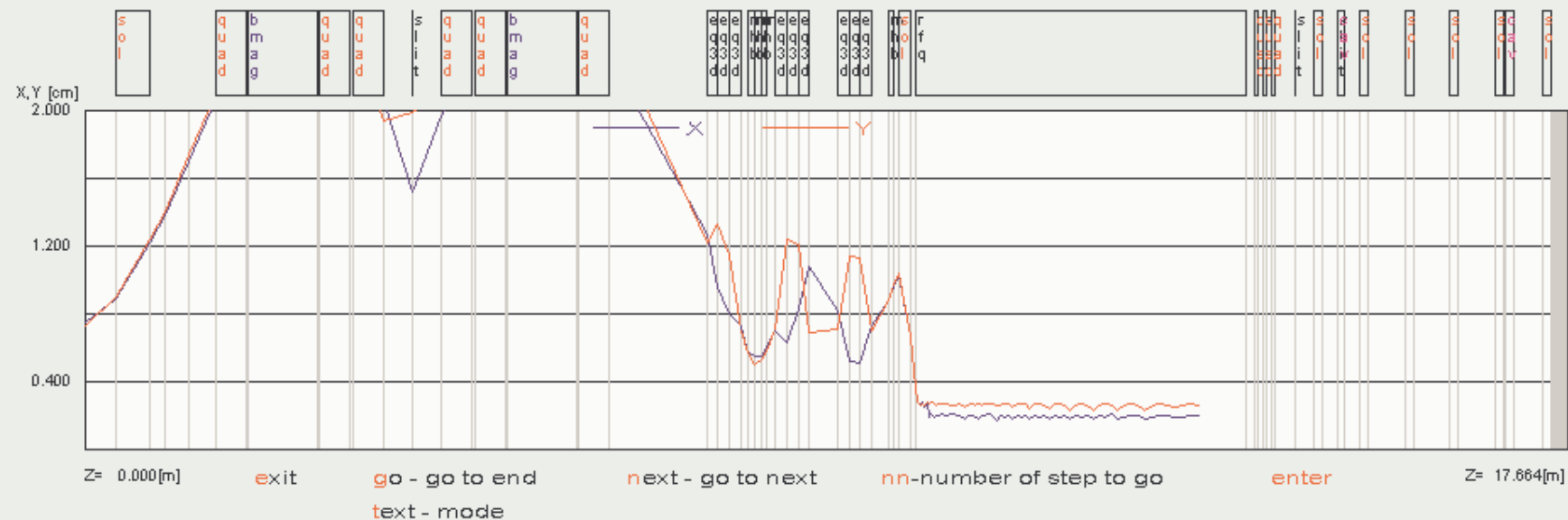
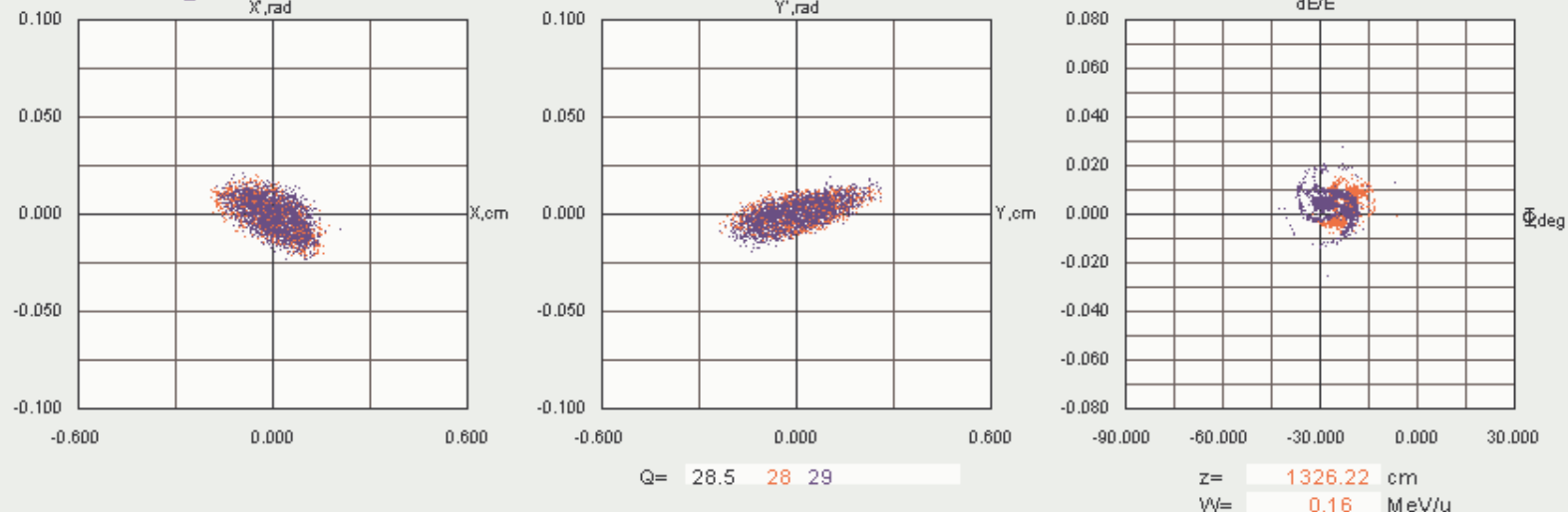
Superconducting Linac



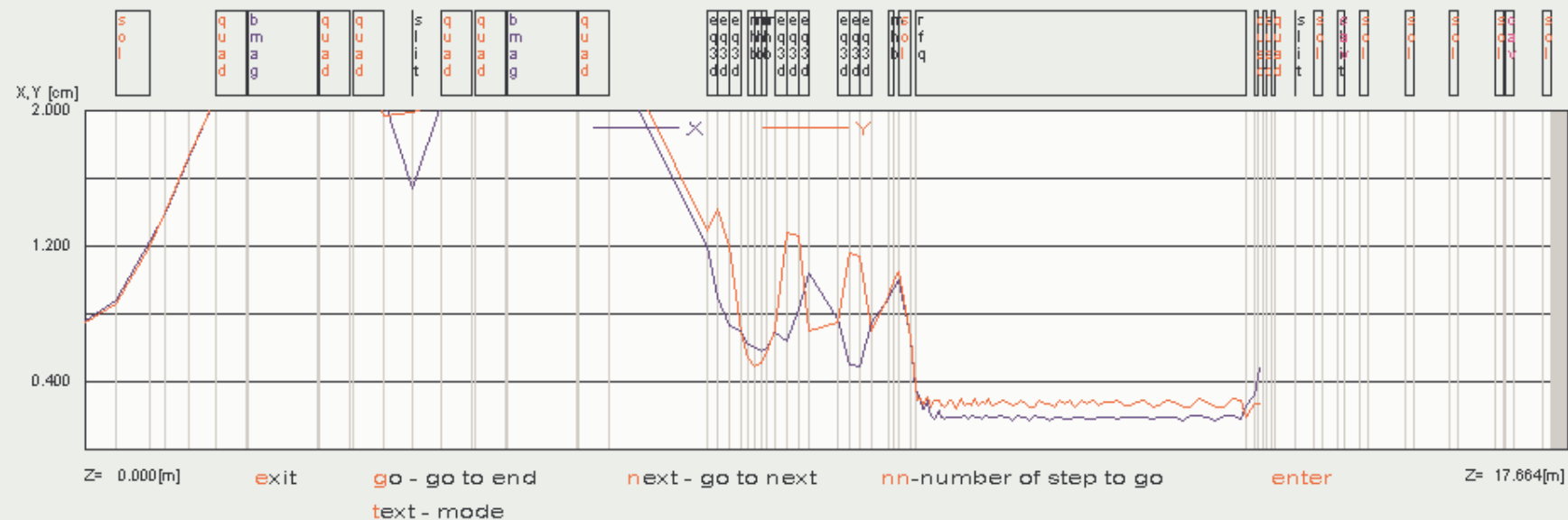
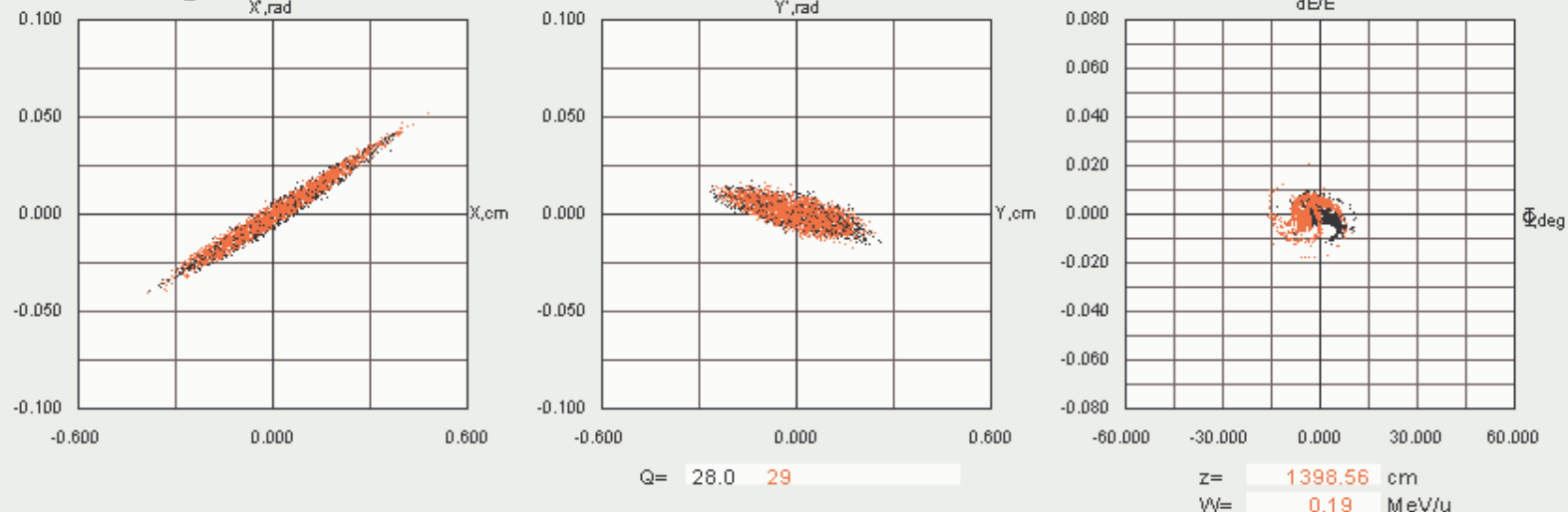
Superconducting Linac



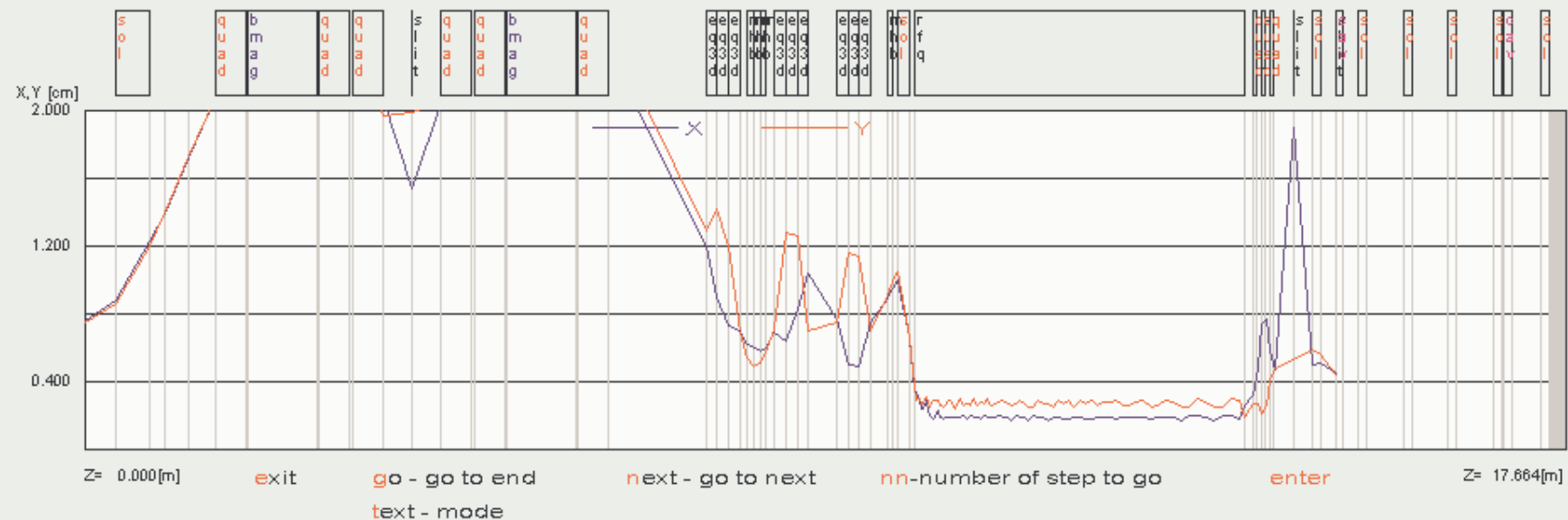
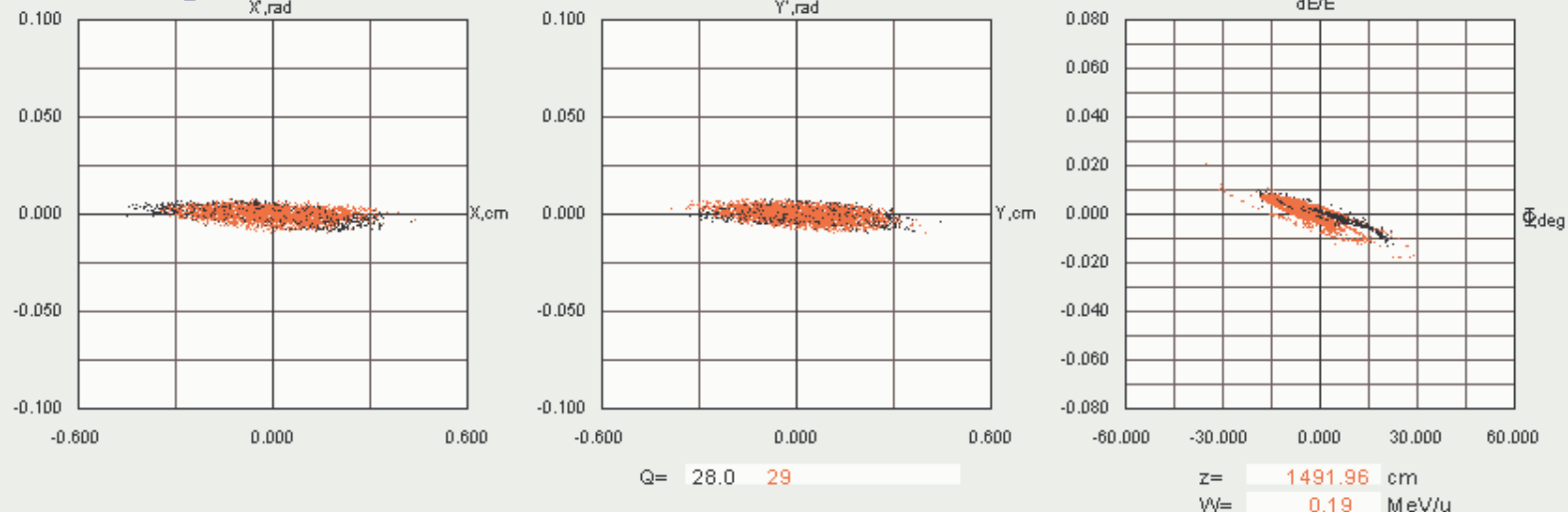
Superconducting Linac



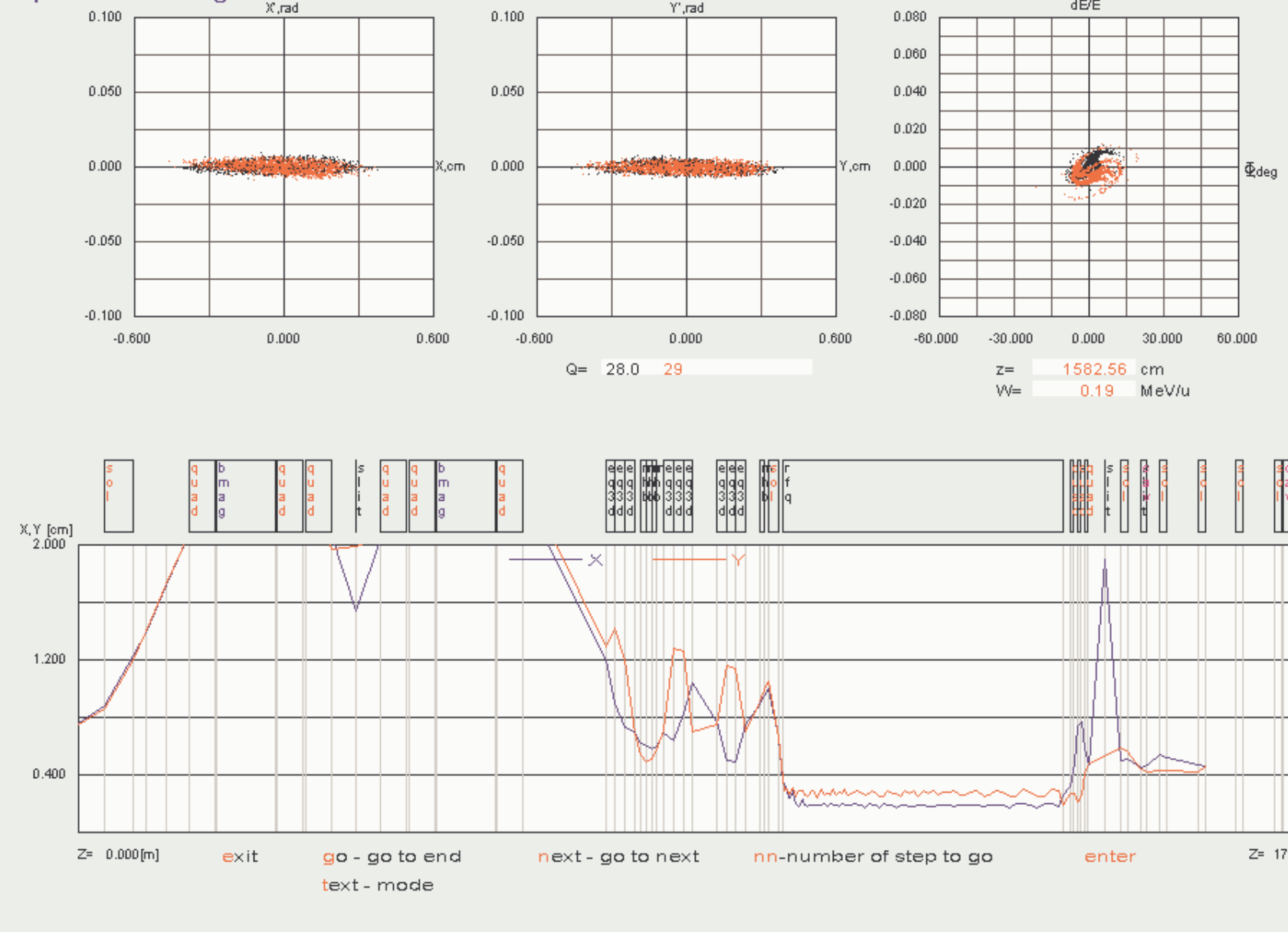
Superconducting Linac



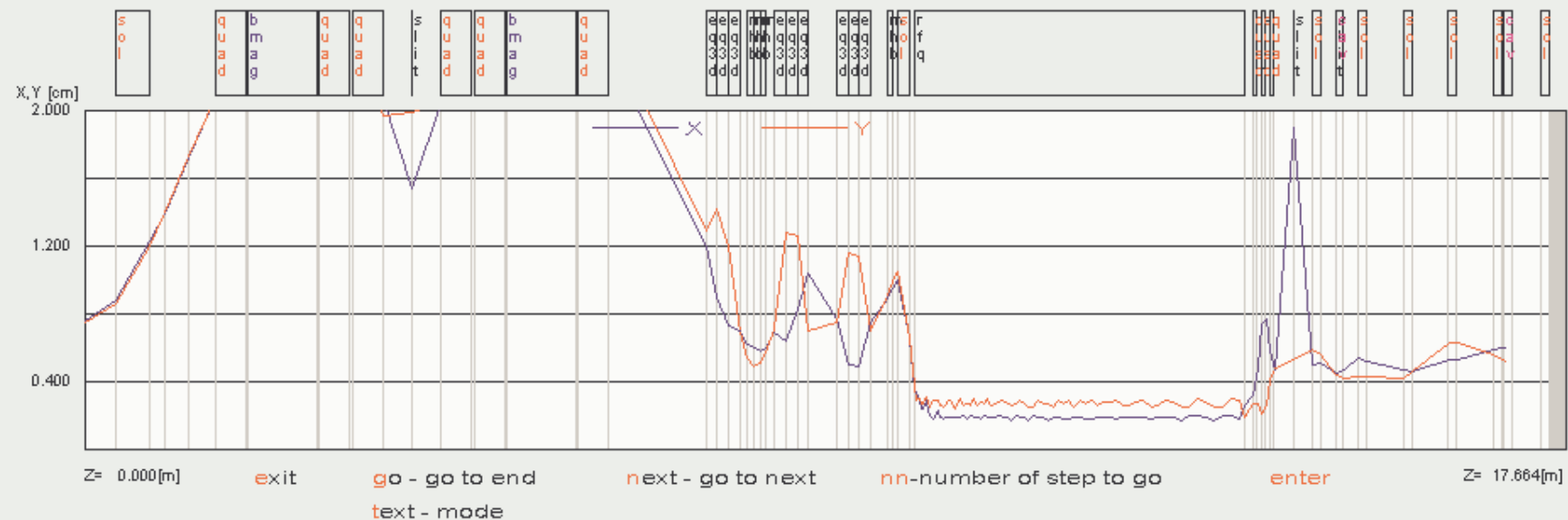
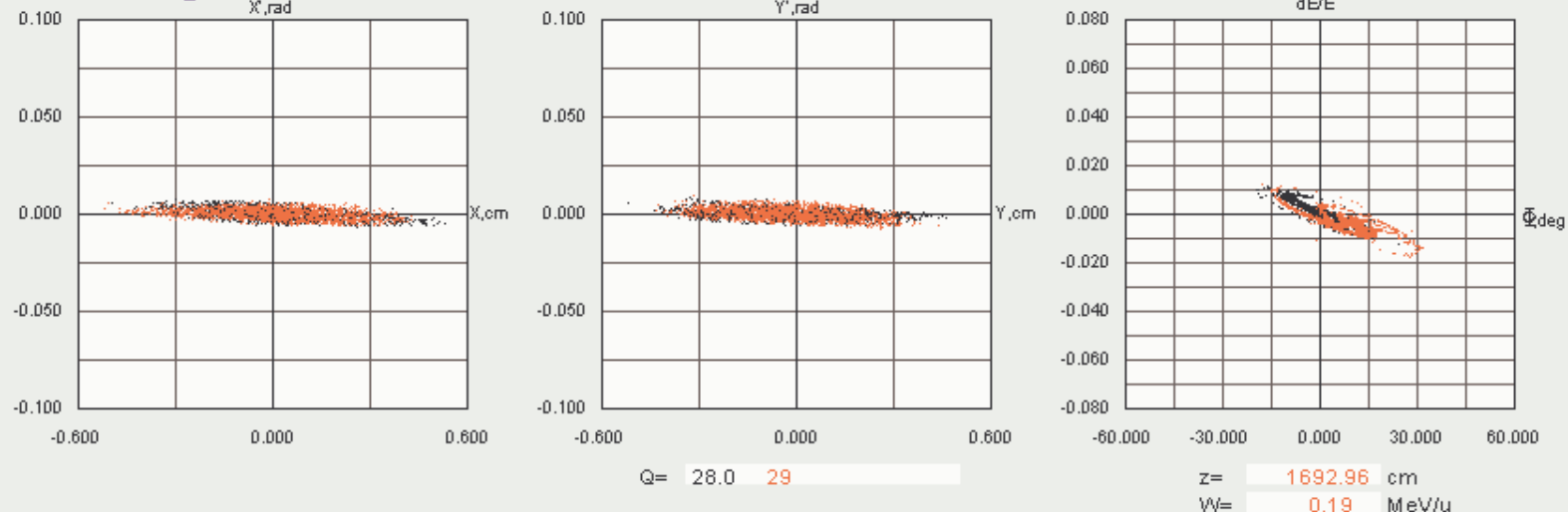
Superconducting Linac

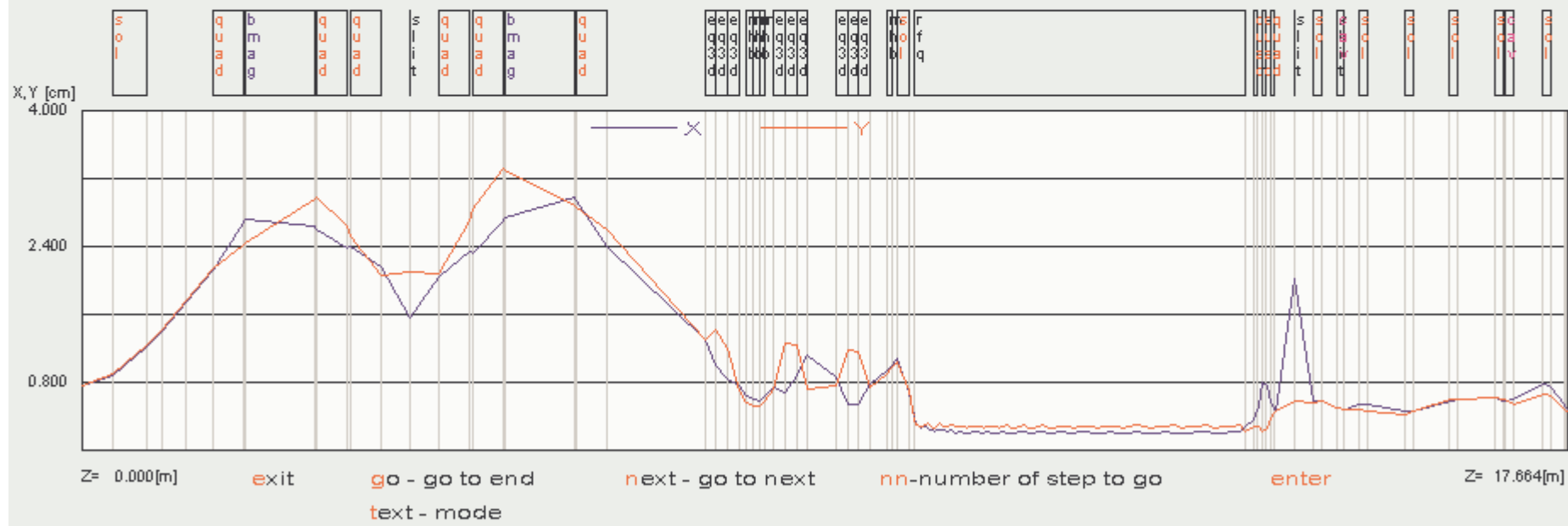
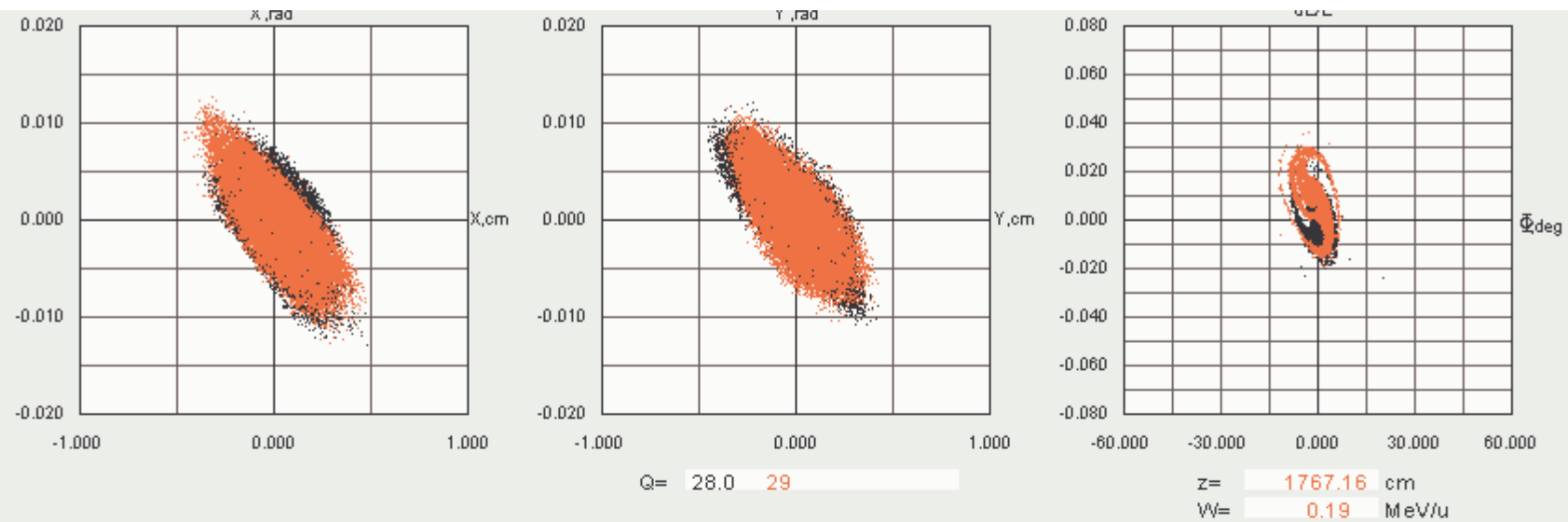


Superconducting Linac

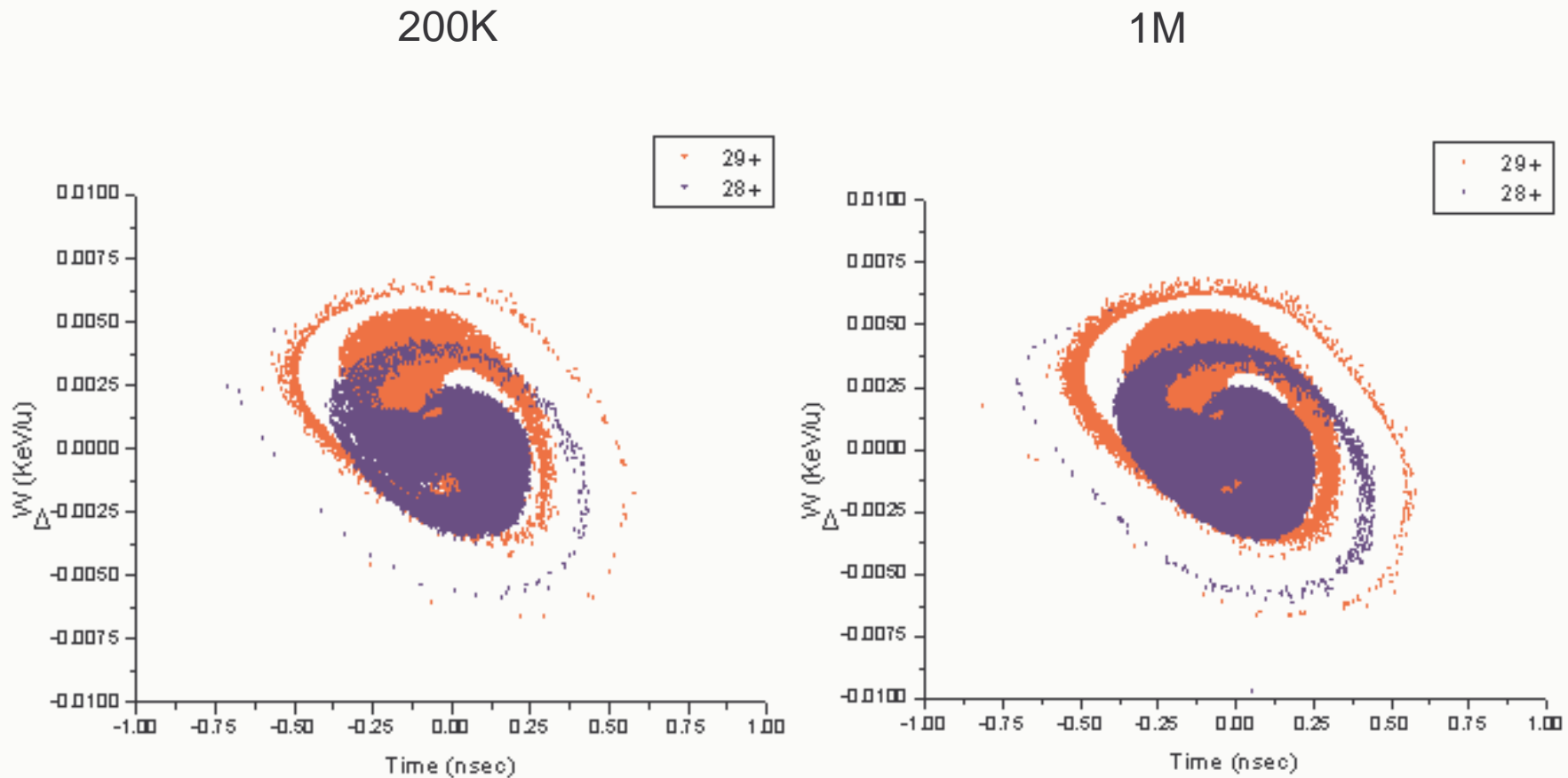


Superconducting Linac

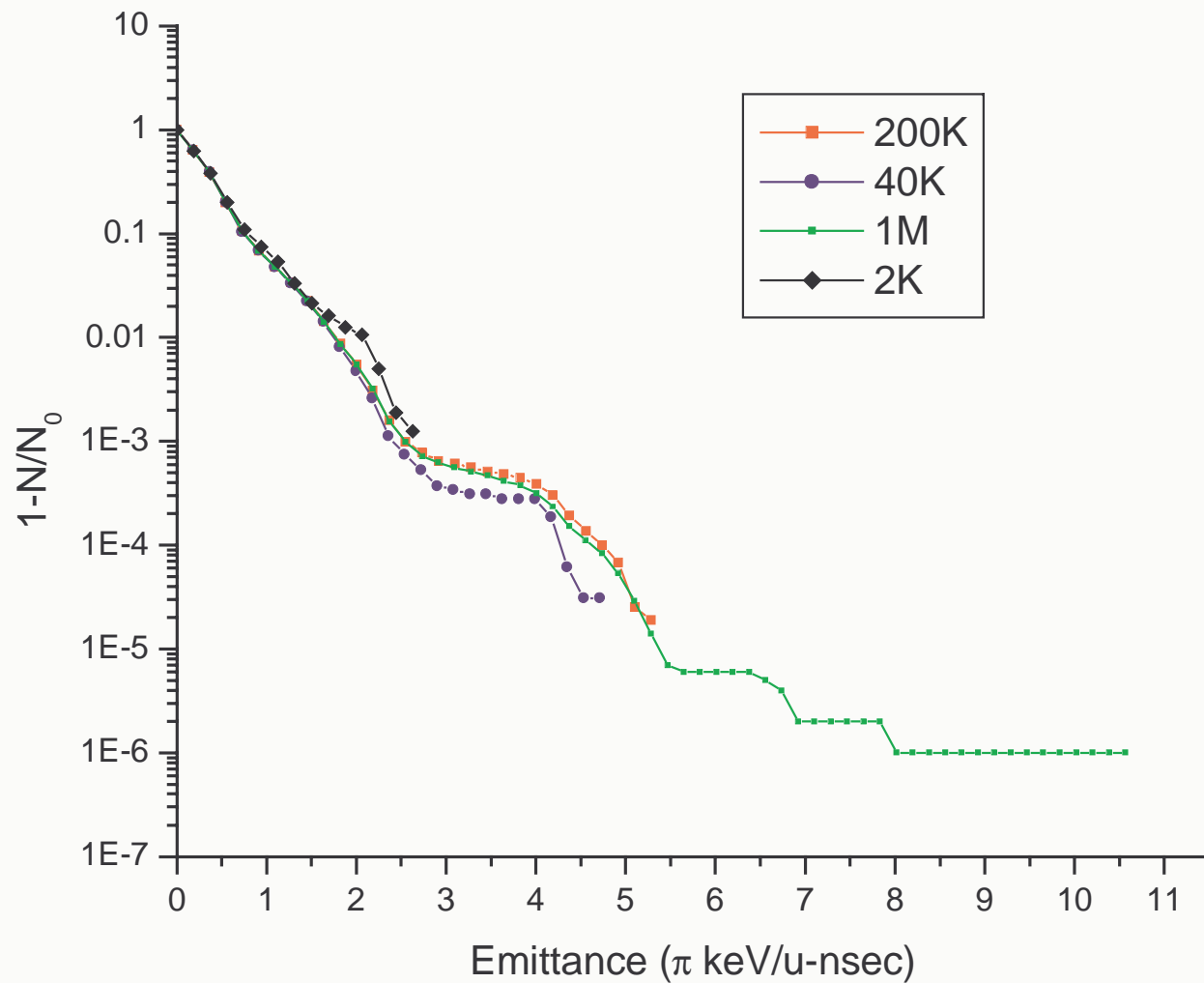




Longitudinal emittance at the entrance of the SC linac



Intensity distribution in the longitudinal phase space

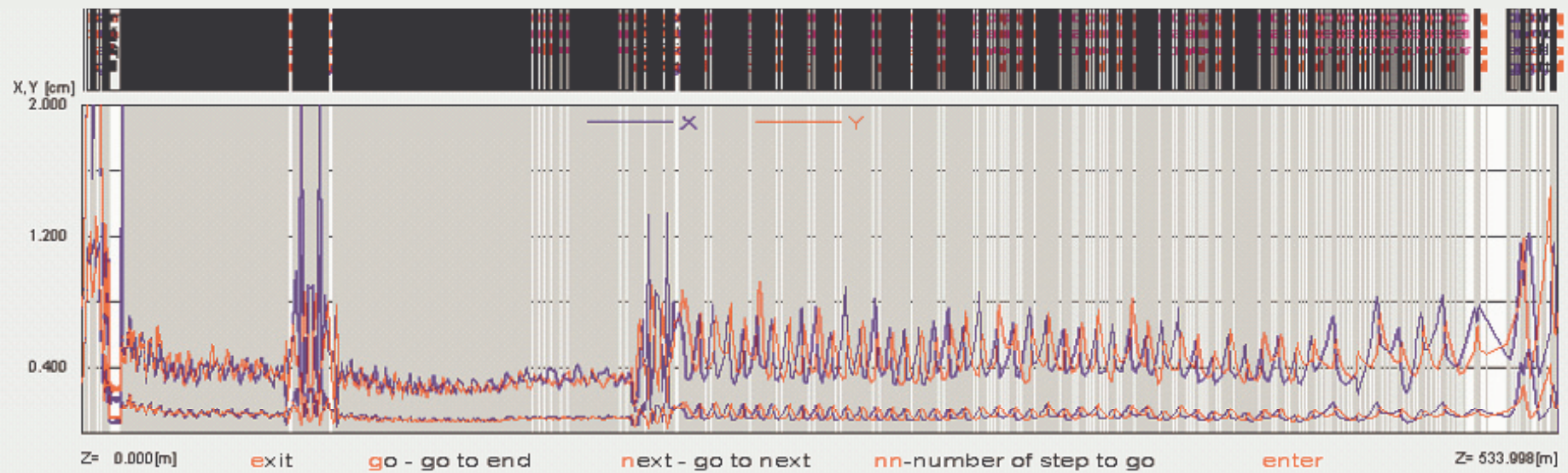
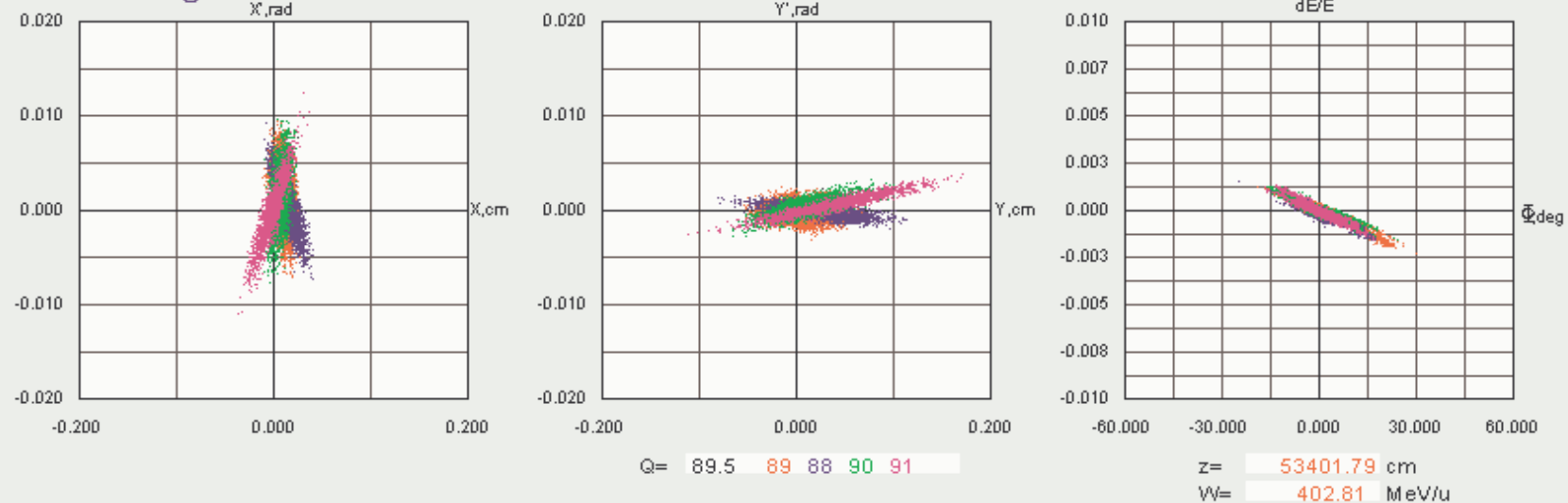


Computer code *TRACK* is being used for BD simulations from ECR-to-Target

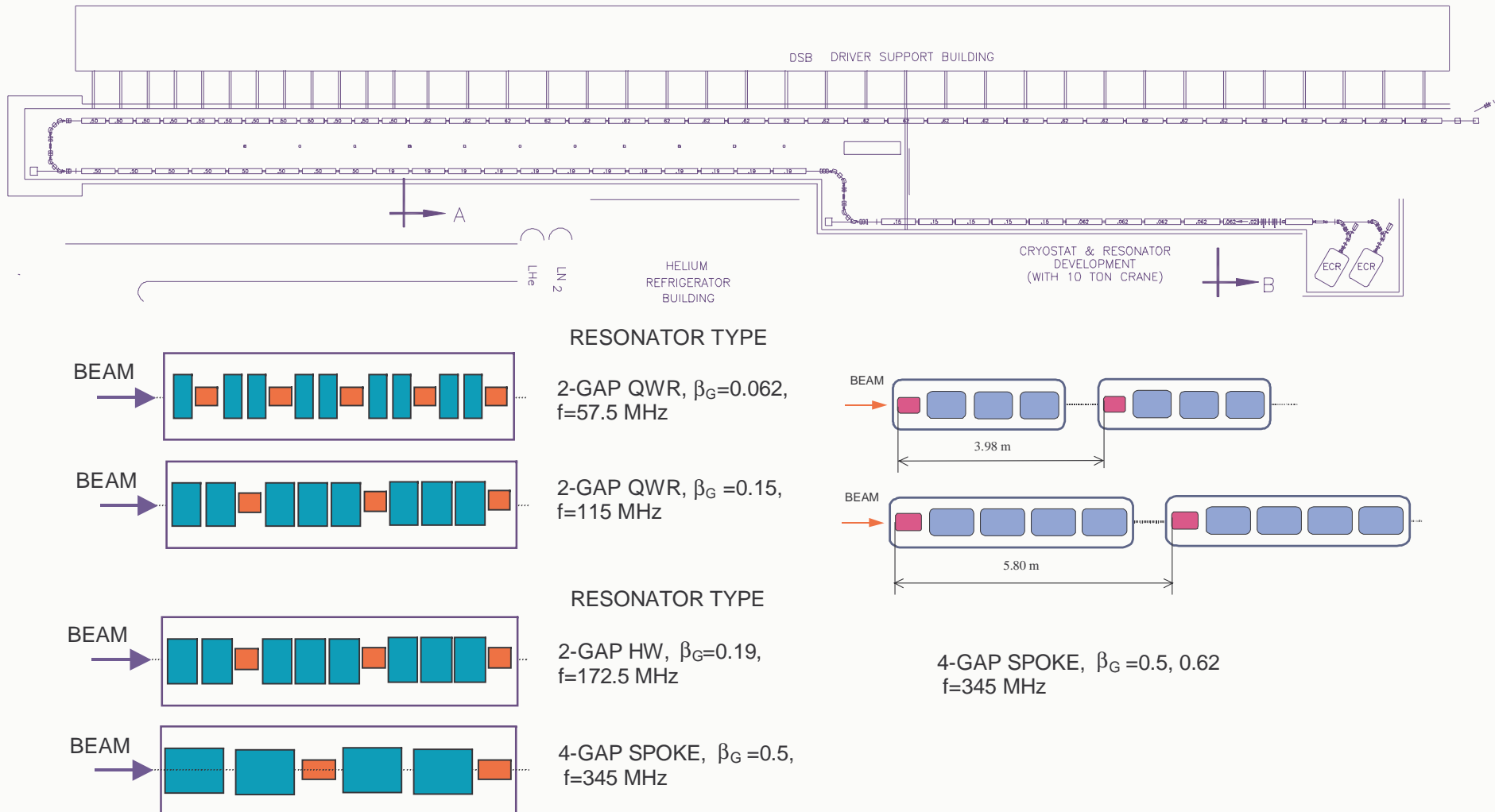
- Integration of particle trajectories of multi-component ion beams in 6D phase space;
- Electrostatic, magnetostatic and electromagnetic fields of all RIA elements are obtained from 3-dimensional external codes.
- Misalignments and random errors are included. Beam steering procedure is applied in the linac with misaligned components.
- Space charge of multiple component ion beams is obtained from 3D Poisson solver.
- Beam passage through stripping foils&films is included; SRIM data of particle distribution in 6D phase space is parameterized.
- Parallel computing on multiprocessor computer cluster JAZZ at ANL. Simulation of total $3.2 \cdot 10^7$ particles requires ~6.5 hours.
LINUX Version of the TRACK is developed by Brahim Mustapha.

ECR-to-Target simulation

Superconducting Linac



RIA Driver Linac



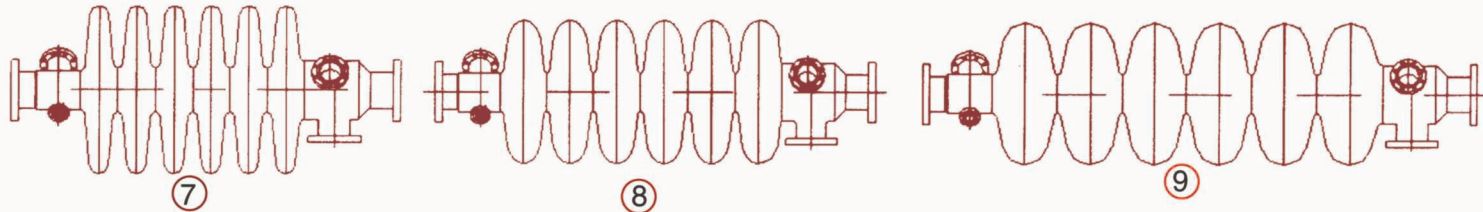
Two options of the high- β section of the driver linac

Elliptical cavities, 805 MHz – ECL – Baseline design

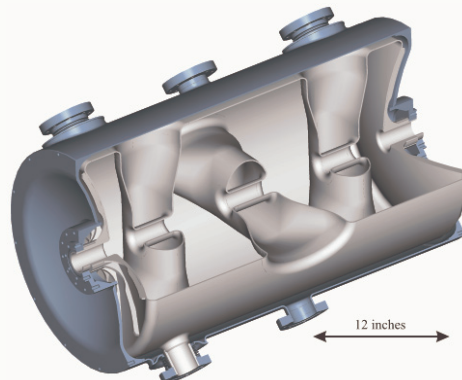
$$\beta_G = 0.47$$

$$\beta_G = 0.6$$

$$\beta_G = 0.81$$



Triple spoke cavities, 345 MHz - TSL



Two types of the TSR:

$$\beta_G = 0.5$$

$$\beta_G = 0.62$$

Beam Loss Studies

- Beam dynamics optimization along the driver linac:
 - ECR-LEBT-RFQ-MEBT including space charge and multi-component ion beams;
 - Different accelerating-focusing lattice (QWR, HWR, TSR, EC);
 - Higher-order optimization of the post-stripper sections.
 - Minimize effective emittance growth of the multi-q beam.
- Simulation in 3D focusing and accelerating fields.
- Include passage of ions through the strippers.
- Effective cleaning of beam halo by collimation in designated areas.
- Simulate 200 seeds with errors and misalignments (automatic steering is applied for static misalignments).
- Register controlled and uncontrolled beam losses.

Passage through the stripper, SRIM results of elastic scattering

U-238 at 85 MeV/u

on

15 mg/cm² carbon
stripper

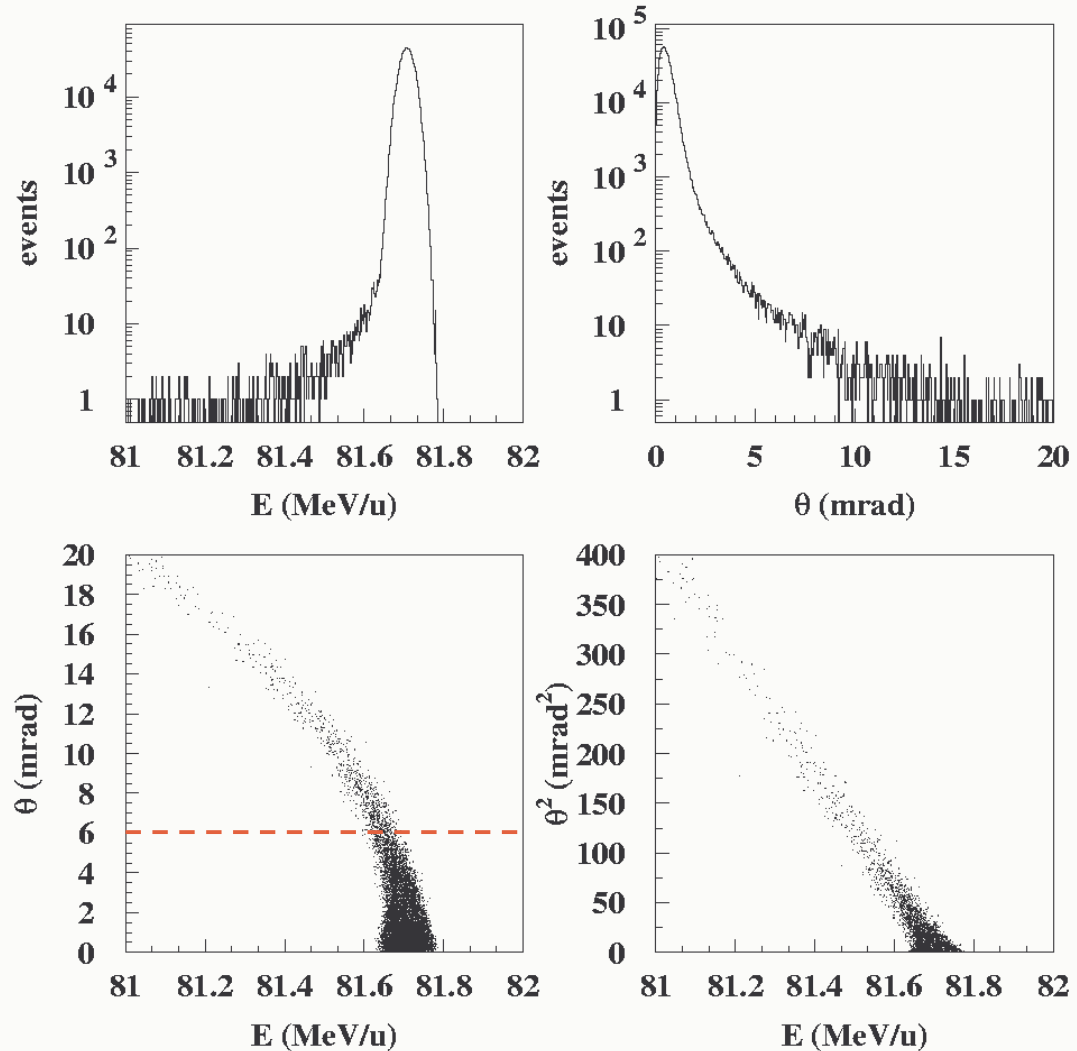
1M events

(~ 1 week on 1.8
GHz PC)

$\Delta W = 3.29 \text{ MeV/u}$

$\sigma_W = 17.6 \text{ keV/u}$

$\sigma_T = 0.5 \text{ mrad}$

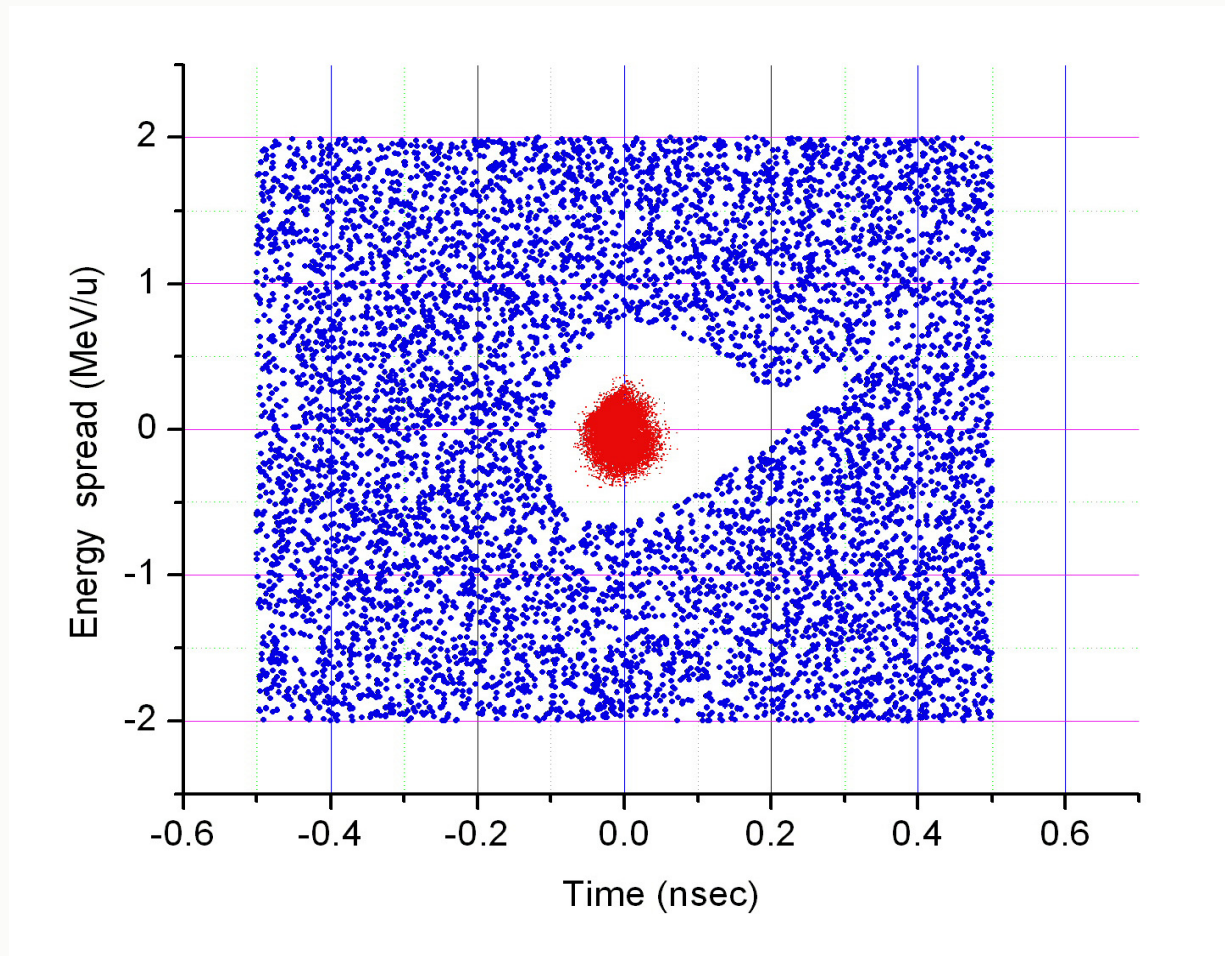


Consequences:

- Thickness fluctuation is an important parameter due to the large ~3.3 MeV/u energy loss.
- Use lower frequency SC resonators. Triple Spoke in the high- β section: larger longitudinal acceptance.
- Collimate beam in the transverse phase space.
- Nuclear reactions: <0.2% of ions, not included. Estimated losses are ~ 10^{-6} . Tracking of radioactive products are required.

Longitudinal acceptance of the ECL

No thickness fluctuation



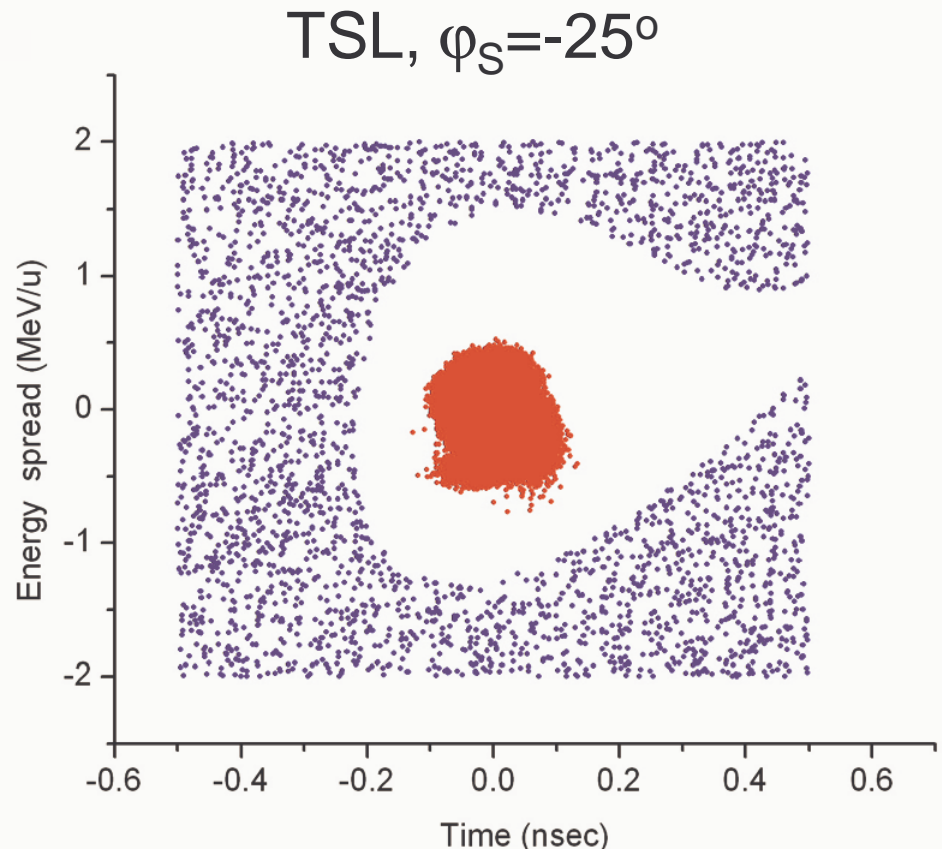
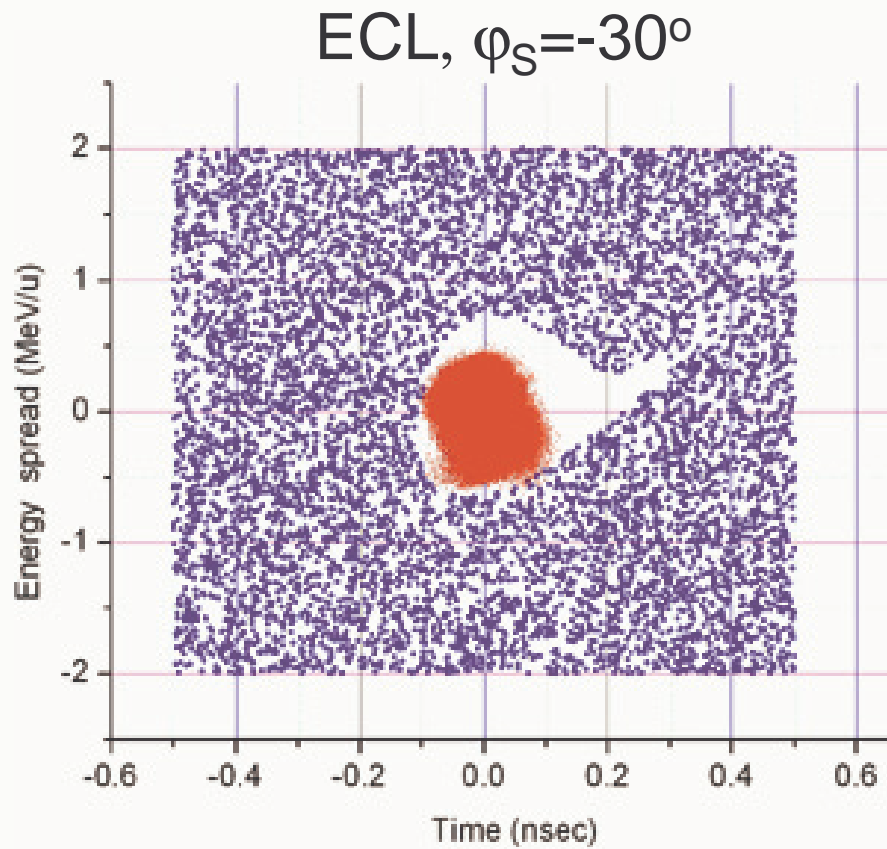
Longitudinal acceptance of ECL and TSL

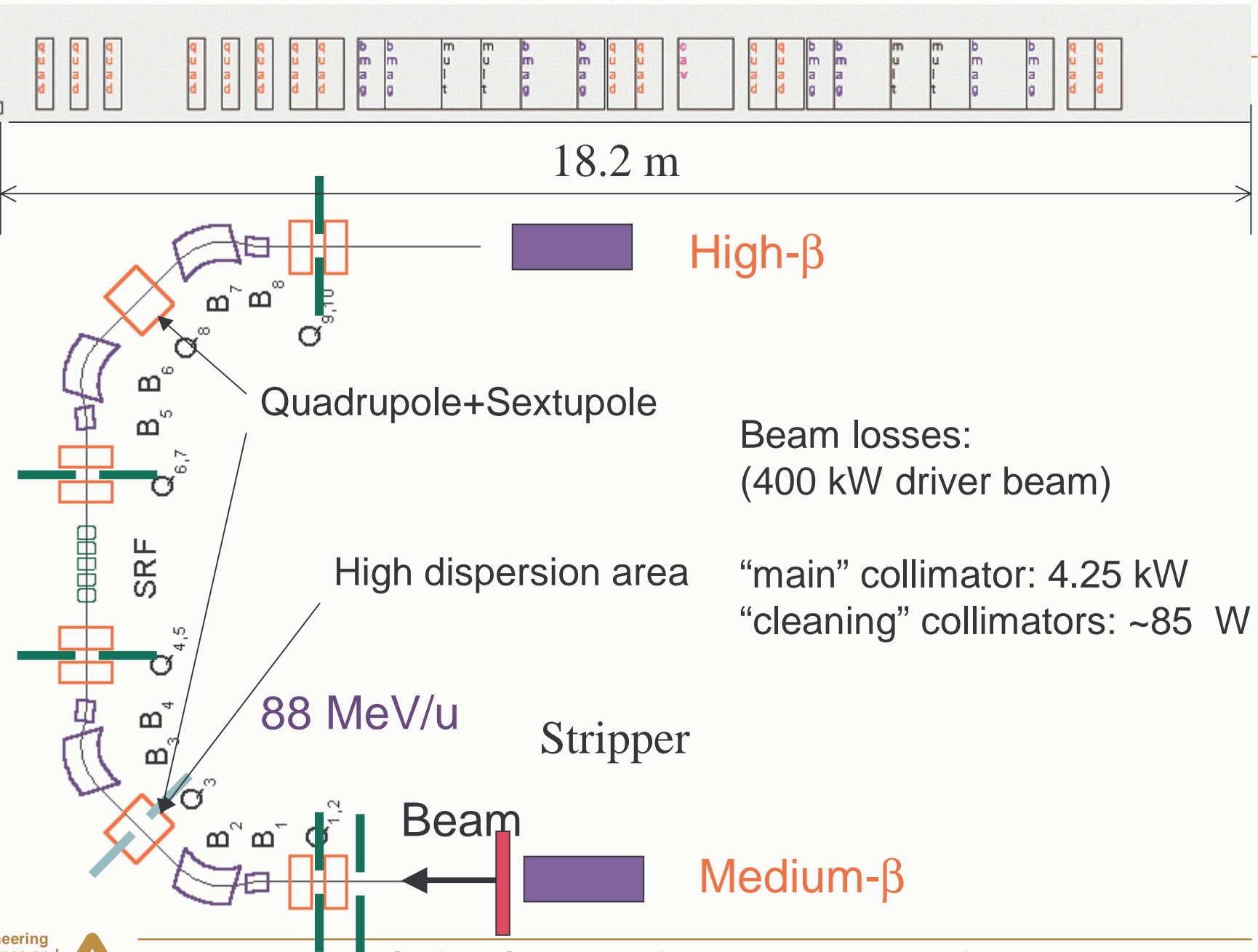
Thickness fluctuation 10%

RF rms errors 0.5% / 0.5%

Misalignments ± 0.5 mm

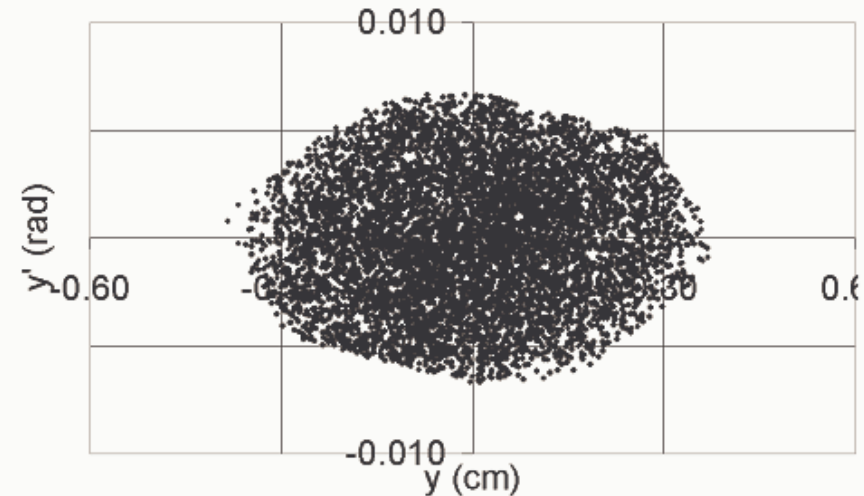
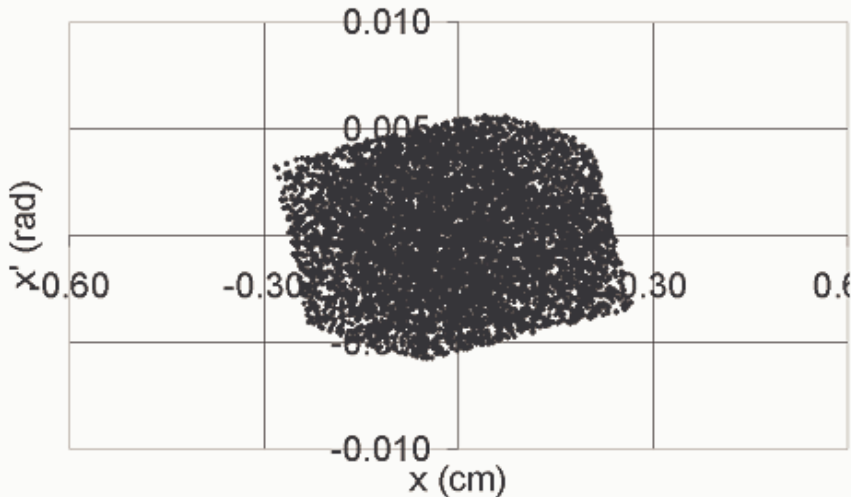
(Steering is applied)





Transverse acceptance with collimators

Slit opening = ± 10 mm



Transverse phase space

Beam rms emittance

$0.2 \pi \text{ mm mrad}$

Acceptance of the MTS
10 mm slit opening

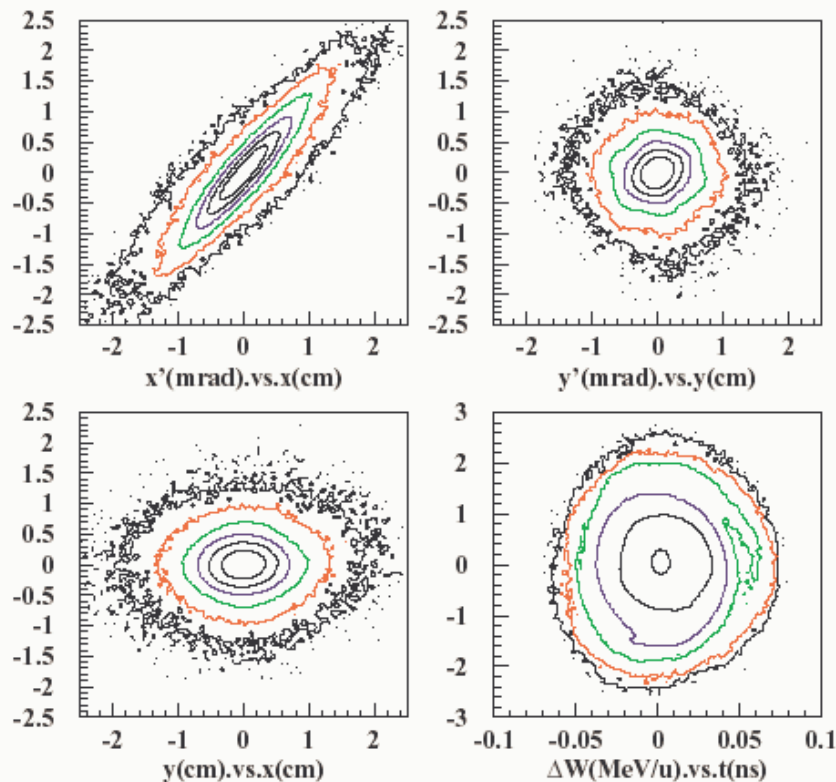
$9.0 \pi \text{ mm mrad} = 45 \cdot \text{rms emittance}$

Beam loss calculations

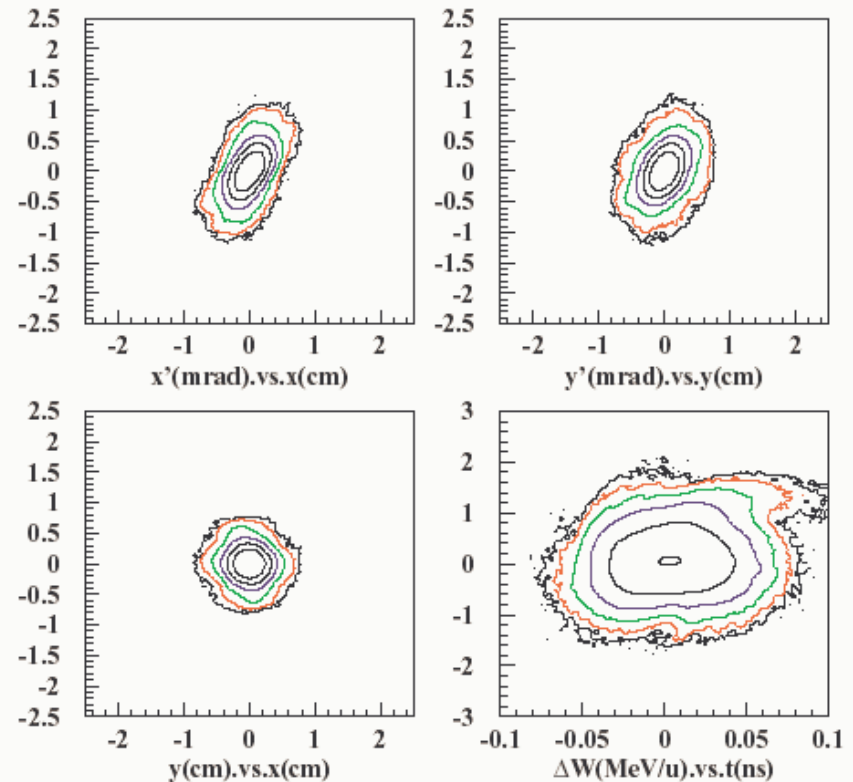
RF (%, deg) rms	Stripper fluc. FWHM (%)	Location	ESL	TSL
0.3	5	MOS-1	$1 \cdot 10^{-3}$	$1 \cdot 10^{-3}$
		MOS-2	$8 \cdot 10^{-4}$	$8 \cdot 10^{-4}$
		High-β	$3.8 \cdot 10^{-4}$	0
0.3	10	MOS-1	$1 \cdot 10^{-3}$	$1 \cdot 10^{-3}$
		MOS-2	$8 \cdot 10^{-4}$	$8 \cdot 10^{-4}$
		High-β	$3 \cdot 10^{-3}$	0
0.5	5	MOS-1	$1 \cdot 10^{-3}$	$1 \cdot 10^{-3}$
		MOS-2	$8 \cdot 10^{-4}$	$8 \cdot 10^{-4}$
		High-β	$5 \cdot 10^{-3}$	0
0.5	10	MOS-1	$1 \cdot 10^{-3}$	$1 \cdot 10^{-3}$
		MOS-2	$8 \cdot 10^{-4}$	$8 \cdot 10^{-4}$
		High-β	$1 \cdot 10^{-2}$	0

Beam data at the exit of linac, image of 32 million particles

Baseline linac



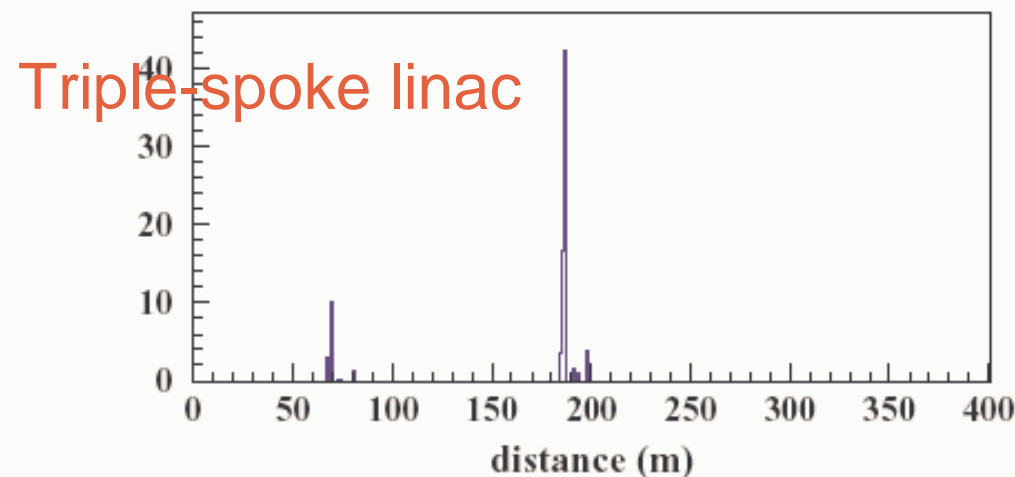
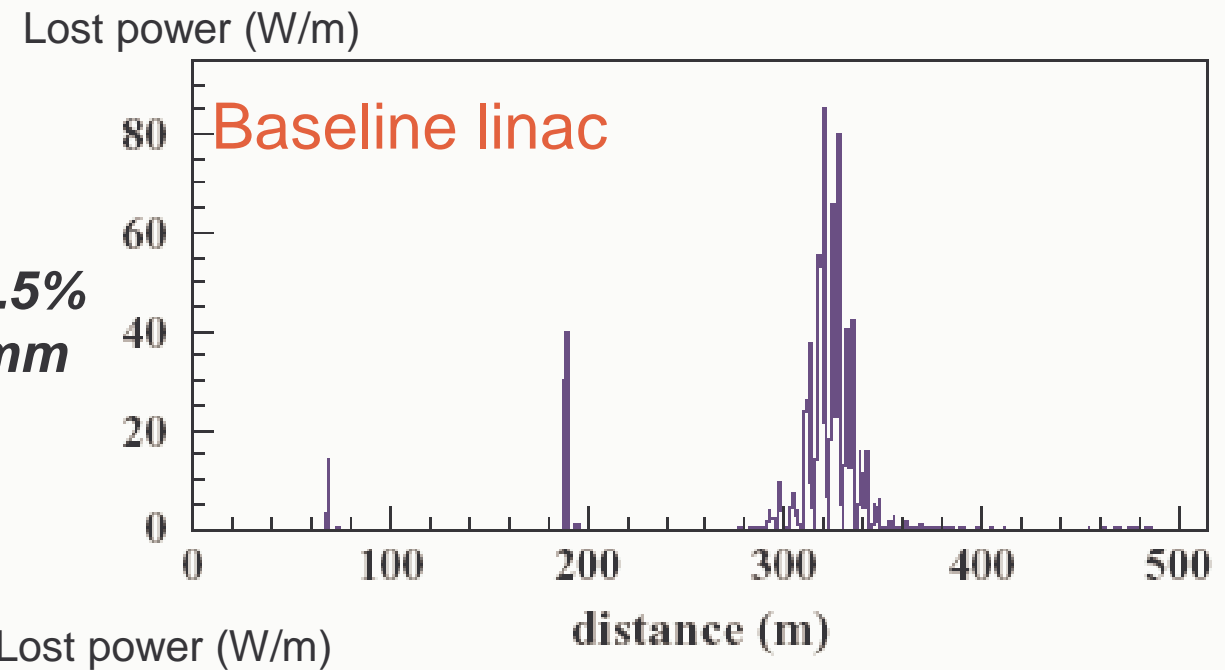
Triple-spoke linac



Note: logarithmic levels of the density isolines

Beam Losses, thickness fluctuation 10%,

Thickness fluct. 10%
RF rms errors 0.5% 0.5%
Misalignments ± 0.5 mm
(Steering is applied)



Conclusion on RIA Driver Linac

- As applied to the RIA driver linac, spoke-loaded cavities provide a number of advantages compared with the higher-frequency, elliptical-cell cavities that have been proposed for this application. In particular, using TEM-class, spoke-loaded cavities:
 - a) Reduces the required number of cavities from 180 to 140.
 - b) Reduces the number of cavity types in the high-energy section from 3 to 2
 - c) Increases the operating temperature from 2 to 4.3 K
 - d) Reduces the refrigeration required by approximately a factor of two.
 - e) Increases the longitudinal acceptance by a factor of 4.7, significantly decreasing the possibilities for beam loss and activation.
 - f) In addition, TEM-class spoke-loaded cavities have excellent mechanical stability, minimizing the difficulty of tuning and phase control.
- Two designs of the driver linac have been compared with respect to the beam losses. The reference design based on elliptical cavities (SNS type) shows significantly higher sensitivity to the linac tuning, rf errors and stripping target quality.

8-GeV linac: evolution from 3-frequency to 2-frequency

RT SNS

TESLA

402

805

1207

TSR: T=4.2K, more economic in operation

RT TSR S-TESLA

TESLA

402

402

1207

1207

- 1) SRF technology is well advanced;
- 2) More economic in operation.

Spoke S-TESLA

TESLA

402

1207

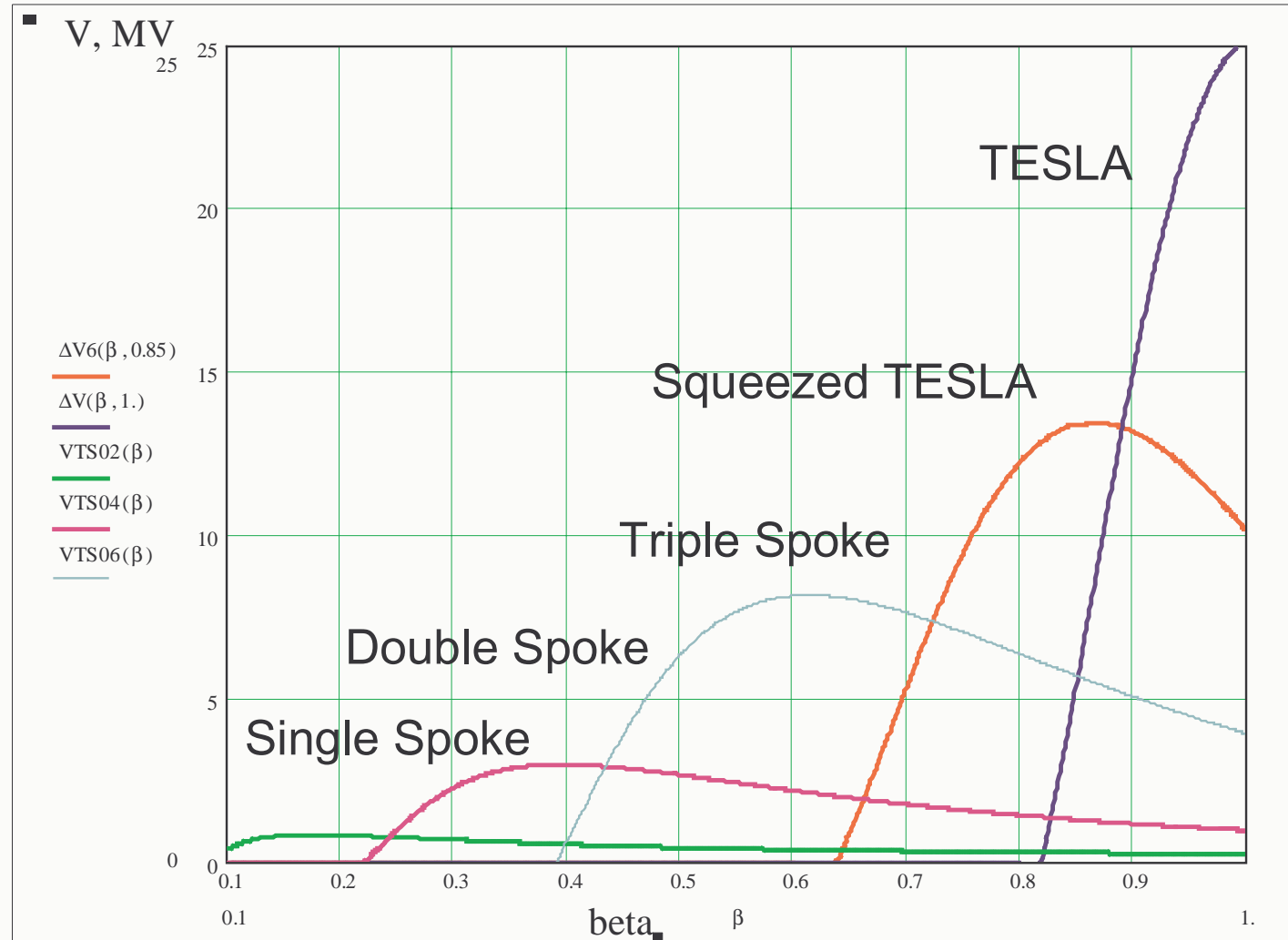
1207

325

1300

1300

8-GeV linac



Single- and double-spoke resonator

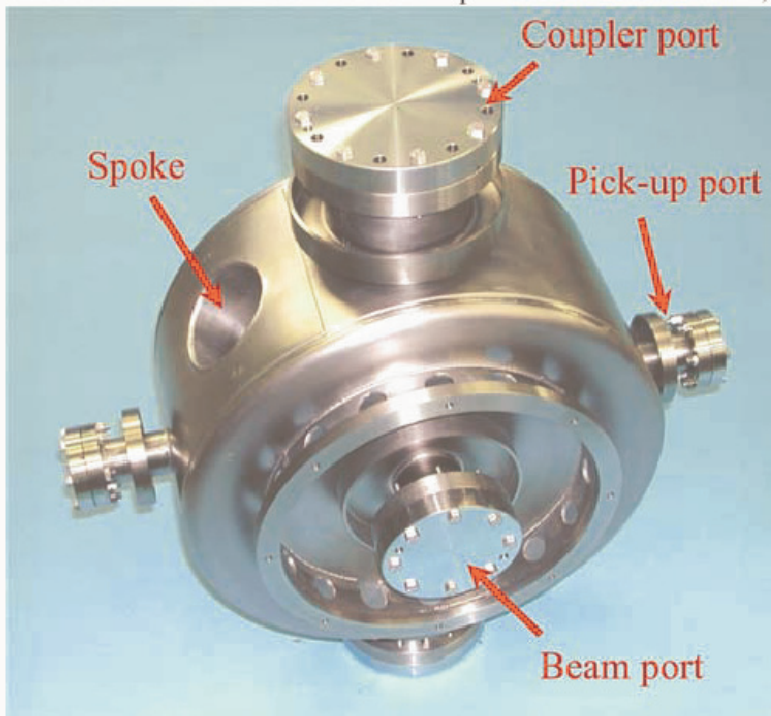


Figure 1: Los Alamos-built 350 MHz, $\beta=0.175$, single-spoke niobium cavity



Figure 5: A 345 MHz, double-spoke, three-gap cavity for $\beta=0.4$. A niobium prototype has been built and tested at Argonne National Laboratory

Triple-spoke resonator

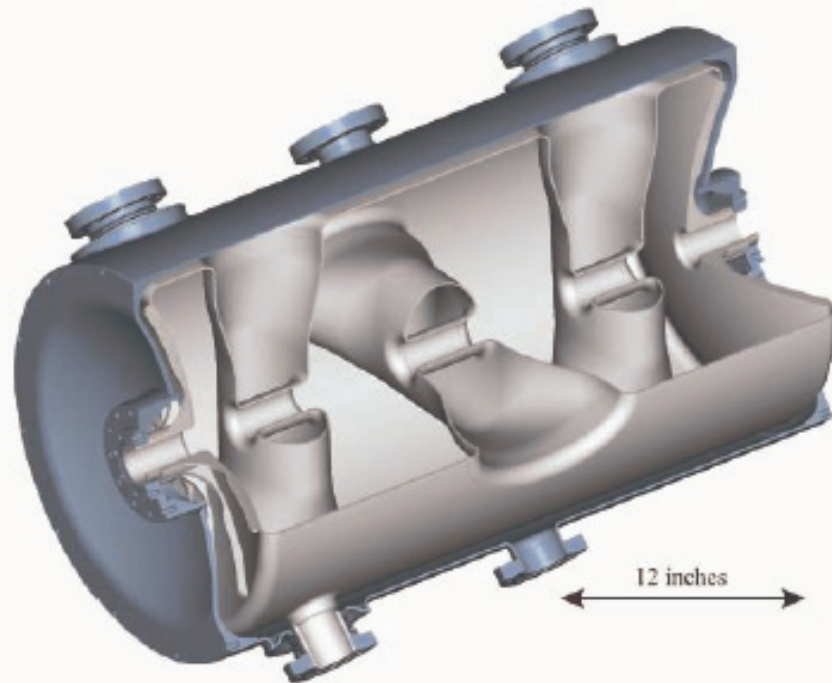
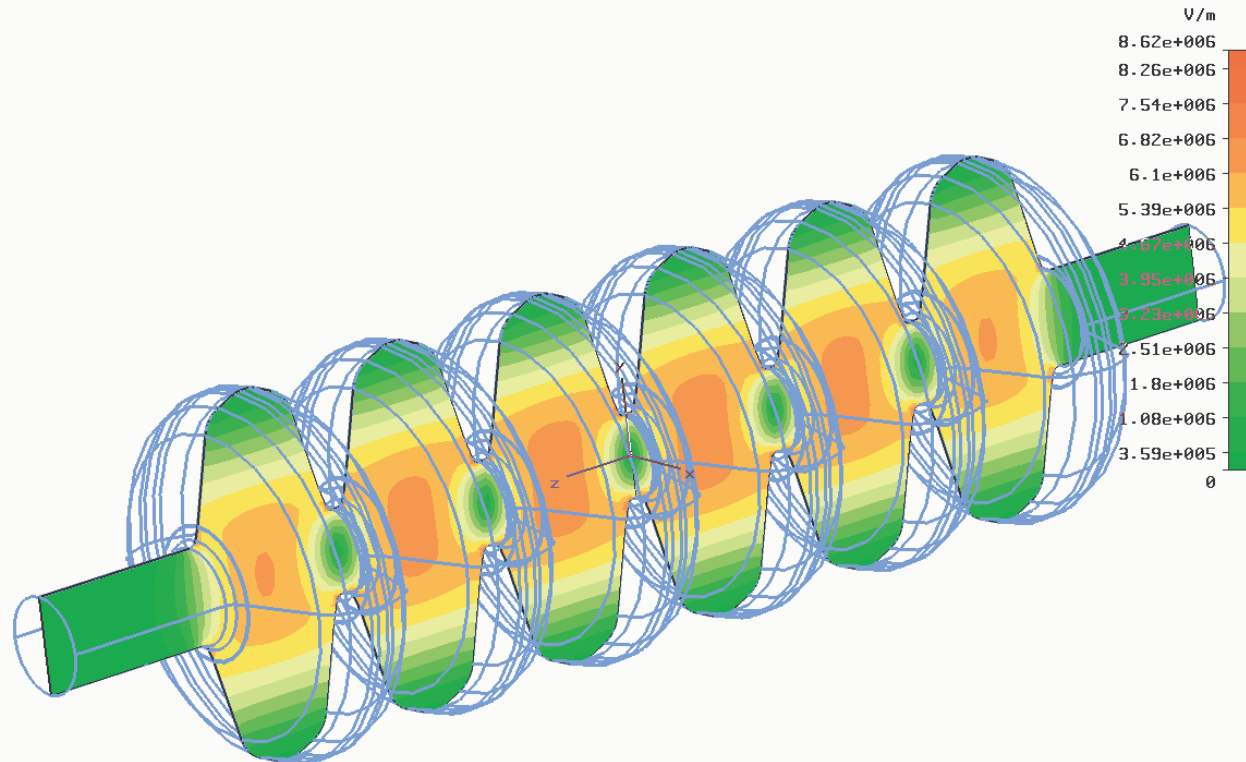


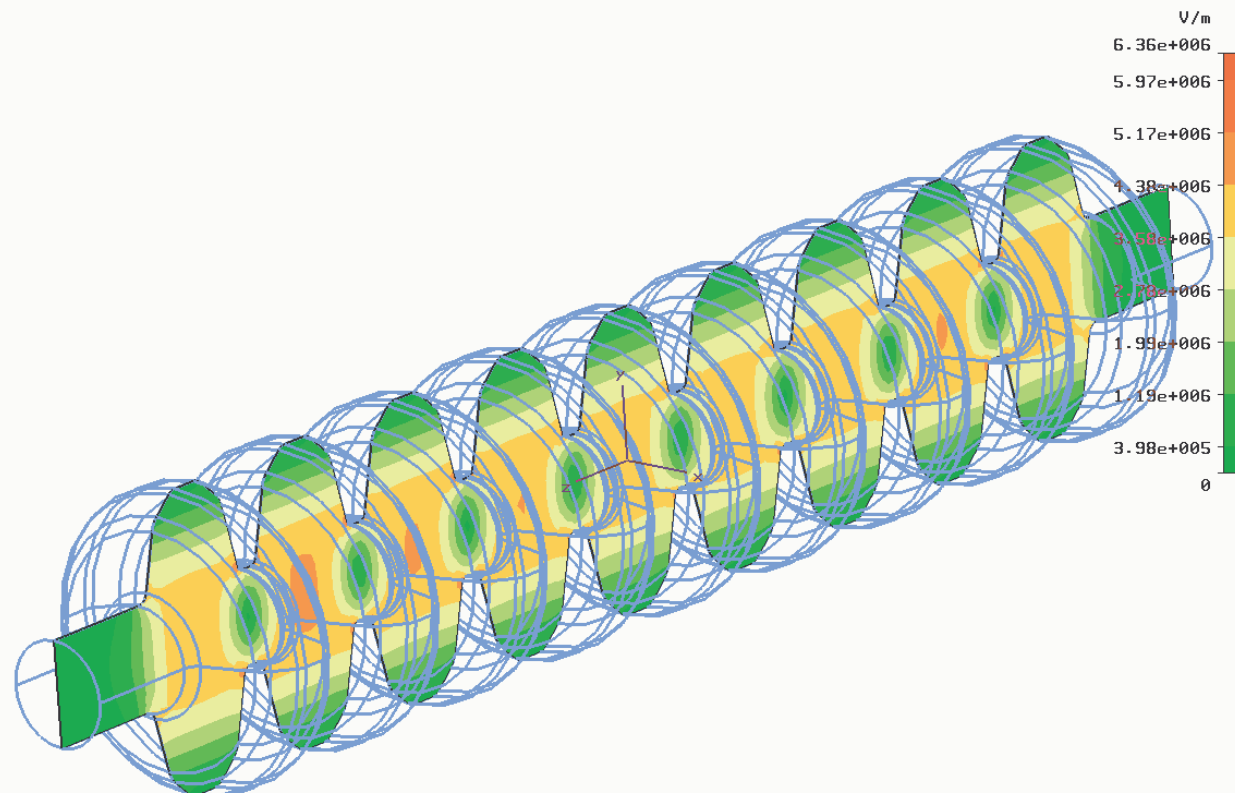
Figure 8: A 345 MHz, $\beta=0.5$ triple-spoke-loaded, four gap accelerating structure. A niobium prototype is under construction at Argonne National Laboratory.

Squeezed 6-cell TESLA



```
Type      = E-Field (peak)
Monitor   = Mode 3
Component = Abs
Plane at x = 0
Frequency = 1206.26
Phase     = 0 degrees
```

TESLA



Linac Lattice

RFQ

Single-spoke and SC solenoids



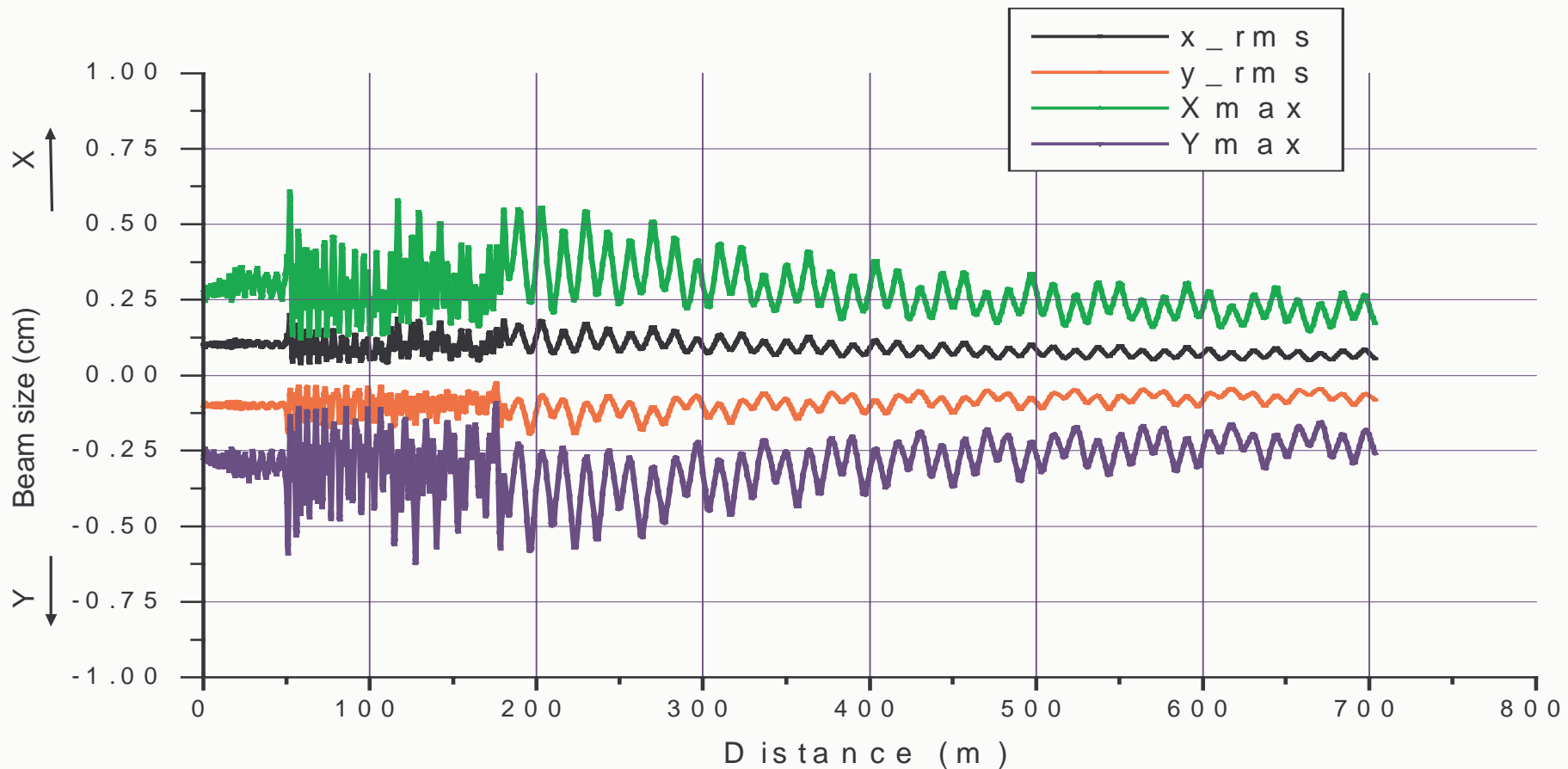
Main parameters of the 8-GeV linac

	SSR	DSR	TSR	S_TESLA	TESLA
Frequency, MHz	402.5	402.5	402.5	1207.5	1207.5
Beta geometrical	0.175	0.366	0.59	0.85	1.0
E_{peak}, MV/m	32	32	35	45	45
E_{peak} / E_{acc}	2.8	3.0	3.0	2.125	2.0
Num. of resonators	36	48	44	68	312
W_{out}, MeV	28.9	121	430	1120	8021
P_{coup}(I=26 mA), kW	20	84	184	317	628
Num. of cav./klyst.	12	12	12	17	12
Num. of klystron	3	4	4	4	26
L_{section}, m	15	35	76	80	550

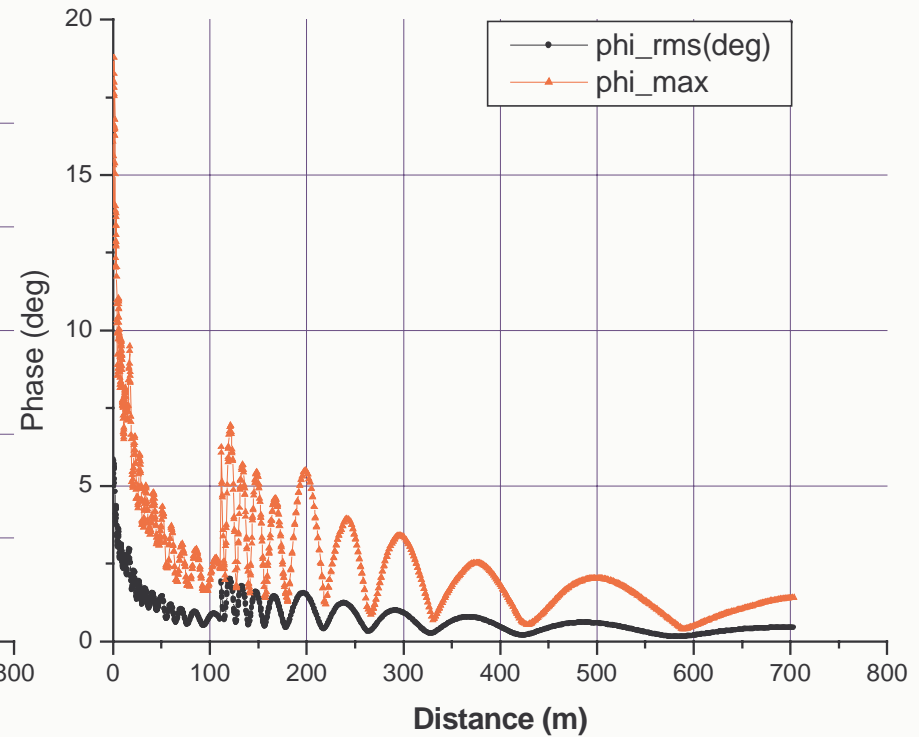
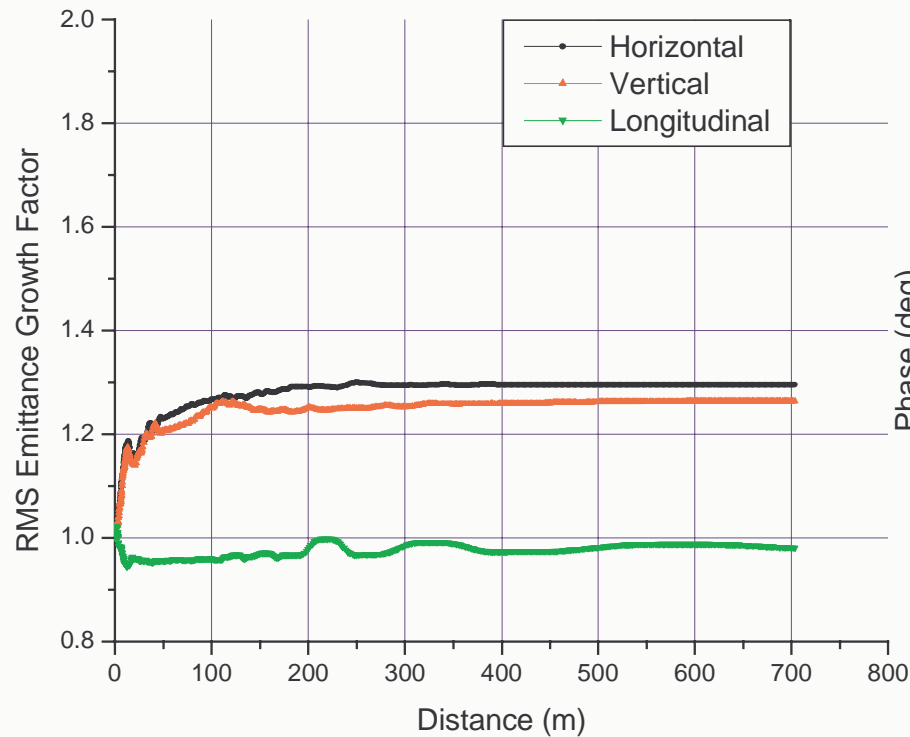
Total number of klystrons 41
 Total number of cavities (402 MHz) 128
 Total number of cavities (1207 MHz) 380

Beam envelope, rms and total

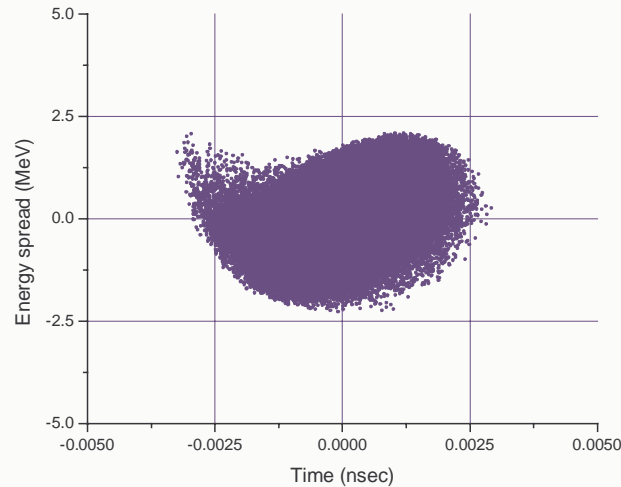
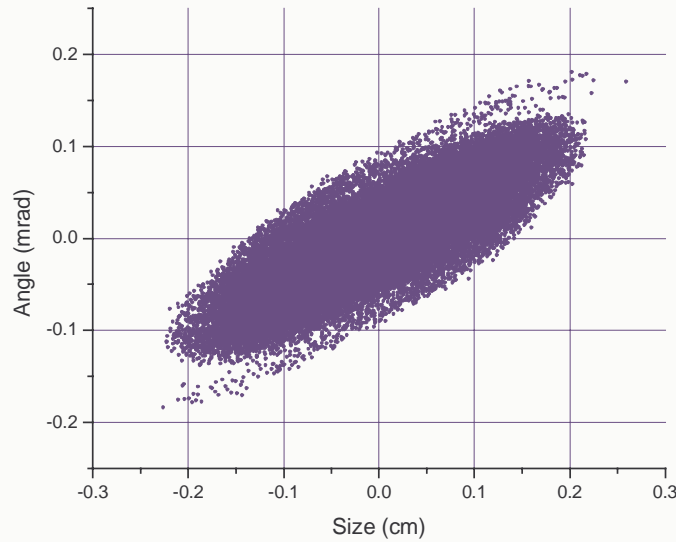
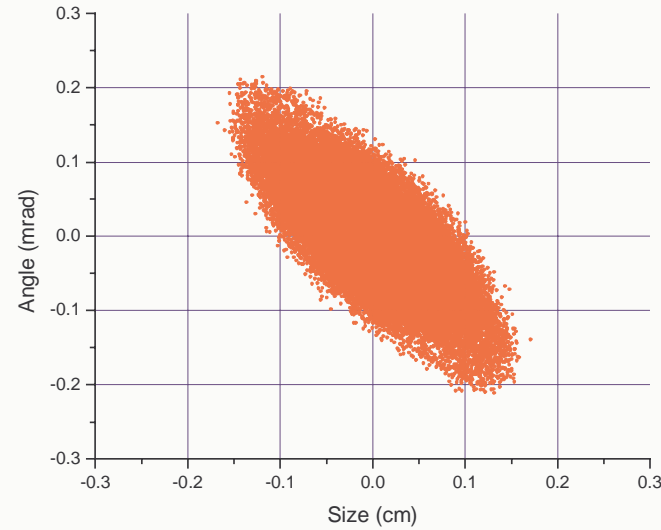
Simulation of $5 \cdot 10^4$ particles



Emittance and phase width evolution



Phase space plots, 8 GeV



- **Advantageous of using two-frequency option of the Linac:**
 - Eliminates room temperature DTLs. Transition from RFQ to SC is at 5 MeV.
 - Lower frequency single- double- and triple-spoke resonators (total 128 resonators) can operate at 4.2 K.
 - Eliminates 805 MHz klystrons and 3 types of elliptical cavities.
 - Slightly higher kinetic energy of electrons compared with the “reference” design. Kinetic energy of electrons is 8.48 GeV compared with 7.84 GeV.
- **Disadvantageous of the two-frequency option:**
 - The number of SC cavities increases from 384 to 508.

Conclusion

- The front end of the high-current multi-GeV proton linac can be based on spoke-loaded resonators.
- 8-GeV linac can be composed from SRF resonators and rf systems operating at TESLA frequency and 3rd or 4th subharmonic frequency.